Am J Transl Res 2024;16(10):5228-5247
www.ajtr.org /ISSN:1943-8141/AJTR0155143

Original Article

Unveiling the oncogenic significance of thymidylate synthase in human cancers

Yibo Geng[1*], Luyang Xie[2*], Yang Wang[1], Yan Wang[1]

[1]Department of Neurosurgery, Beijing Chaoyang Hospital, Capital Medical University, Beijing, China; [2]Department of Neurosurgery, Beijing Tiantan Hospital, Capital Medical University, Beijing, China. [*]Equal contributors.

Received December 27, 2023; Accepted August 26, 2024; Epub October 15, 2024; Published October 30, 2024

Abstract: Objective: Thymidylate synthase (TYMS) constitutes a pivotal and potent target in the context of chemoresistance. However, the oncogenic role of TYMS has received insufficient attention. Methods: Leveraging data from the Cancer Genome Atlas (TCGA) and various public databases, we conducted an extensive investigation into the oncogenic role of TYMS across 33 cancer types. Subsequently, TYMS was inhibited using small interfering RNA (siRNA) in four different cell lines, and cell proliferation and migration were assessed using CellTiter-Glo and Transwell assays. Results: TYMS exhibited pronounced expression across a spectrum of cancers and demonstrated associations with clinical outcome in diverse cancer patient cohorts. Furthermore, genetic alterations were identified as potential influencers of overall survival in specific tumor types. Notably, the expression of thymidylate synthase correlated with tumor-infiltrating CD4+ cells in select cancers. Additionally, the functional mechanism of TYMS encompassed nucleotidase activity, chromosome segregation, and DNA replication progress. *In vitro* experiments further substantiated these findings, demonstrating that the suppression of TYMS impeded the cell growth and invasive capabilities of HeLa, A549, 786-O, and U87_MG cells. Conclusions: This study furnishes a comprehensive understanding of the oncogenic role played by TYMS in human tumors.

Keywords: Thymidylate synthase, tumor, TGCA, prognosis, tumor-infiltrating immune cell

Introduction

The exploration of novel oncogenes is crucial for achieving a comprehensive understanding of the mechanisms underlying malignant tumors and identifying therapeutic targets [1]. Using resources such as TCGA and various other publicly available analysis websites, which house valuable genomics and proteomics information [2], facilitates interactive analysis specifically focused on unraveling the oncogenic role of TYMS.

TYMS, a human nucleotide enzyme, plays a pivotal role in endogenous thymidylate synthesis, enabling *de novo* production of thymidylate. TYMS has been extensively studied in contexts such as hepatitis, rheumatic diseases, and neural development [3-5]. Elevated levels of TYMS mRNA and protein have been associated with worse prognosis for a wide range of hematologic and solid tumors [6]. Additionally, thousands of publications on PubMed link elevated TYMS levels in tumors to anti-cancer drug resistance and worse clinical outcome [7-9]. However, few studies have analyzed these articles to reveal the carcinogenic mechanisms of TYMS. This paper synthesizes findings from laboratory-based experiments involving cell or animal models, elucidating the intricate relationship between TYMS and various malignancies, including pancreatic, colorectal, ovarian, breast, esophageal, lung, kidney and skin tumors (**Figure 1**; Supplementary Table 1) [10-26].

In our study, we used data from public databases to conduct a pan-cancer analysis of TYMS, covering gene expression, survival rate, genetic alterations, phosphorylation sites, immune cell infiltration, and related gene functions. Additionally, we conducted cell experiments involving the knockdown of TYMS to elucidate further its oncogenic features across different

https://doi.org/10.62347/IRUZ1011

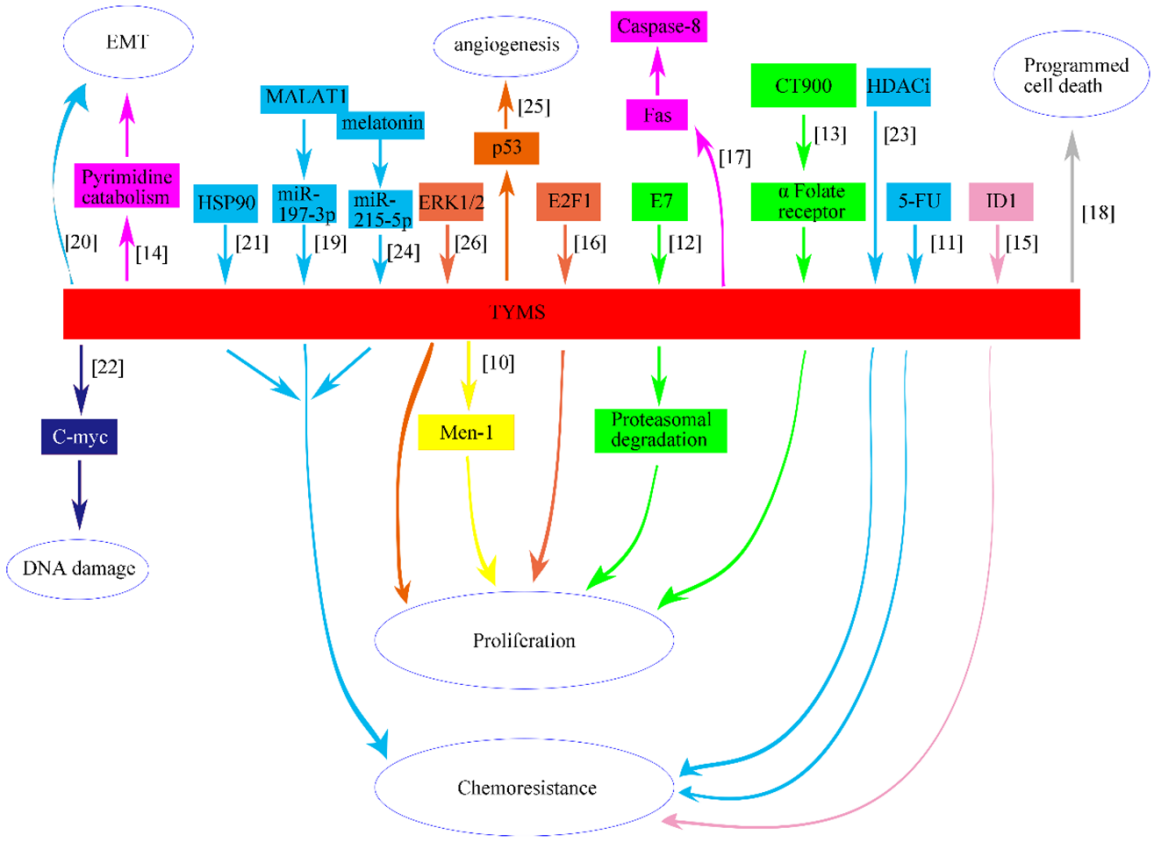

Figure 1. Schematic depicting the relationship between TYMS and eight different types of human cancer, including pancreatic (yellow), colorectal (blue), ovarian (green), breast (pink), esophageal (carneose), lung (brown), kidney (grey) and skin tumor (dark blue).

tumors. This comprehensive approach aims to provide a detailed understanding of the oncogenic mechanisms governed by TYMS.

Materials and methods

Gene location and protein structure analysis

The genomic location of the TYMS gene was determined based on the UCSC genome browser (GRCh38/hg38) [27]. Using the "HomoloGene" function of the National Center for Biotechnology Information (NCBI), conserved functional domain analysis of the TYMS protein across different species was conducted. The three-dimensional structure of TYMS was obtained using the cBioPortal web tool [28].

Gene expression analysis

Tumor Immune Estimation Resource, version 2 (TIMER2): Differences in TYMS expression were assessed using the "Gene_DE" module of the TIMER2 [29]. In cases lacking contrast tissues or a sufficient contrast group, the Gene Expression Profiling Interactive Analysis, version 2 (GEPIA2) web server from Genotype-Tissue Expression (GTEx) was employed [30]. Violin plots depicting TYMS expression across various pathologic stages were generated using the "Pathological Stage Plot" module in GEPIA2, utilizing $\log_2$ [TPM (Transcripts per million) +1] transformed expression results with a log-scale test.

The Human Protein Atlas (HPA): HPA database provided TYMS expression data in different cells, tissues, and plasma [31]. Plasma sample data were estimated through mass spectrometry-based proteomics, defining "low specificity" as "Normalized expression ≥1 in at least one tissue/cell type, but not elevated in any tissue/cell type". Immunohistochemistry (IHC) images of TYMS in five pairs of normal and tumor tissues (breast invasive carcinoma (BRCA), colon adenocarcinoma (COAD), liver hepatocellular carcinoma (LIHC), and lung adenocarcinoma

(LUAD)) were downloaded from HPA and analyzed.

Survival analysis

Using the Kaplan-Meier "Survival Map" module in GEPIA2, overall survival (OS) and disease-free survival (DFS) maps for TYMS were obtained. The expression threshold for categorizing high/low expression groups was set at 50%. Kaplan-Meier survival analysis in GEPIA2 generated survival plots using the log-rank test.

Genetic alteration analysis

Genetic alteration features, alteration frequency, mutation type, and mutated site information for TYMS were collected from the cBioPortal web. OS data for tumors with or without TYMS genetic alterations were collected, and Kaplan-Meier analysis with log-rank *P*-values was performed.

Phosphorylation features

The predicted phosphorylation features of TYMS at sites S6, T53, S114, S124, Y146, S151, Y153, S154, and T167 were obtained from the open-access PhosphoNET database by searching the protein name "TYMS".

Immune infiltration cell analysis

The association between TYMS expression and immune infiltrates, specifically CD4+ T-cells, CD8+ T-cells, cancer-associated fibroblasts, and natural killer (NK) cells, was explored using the TIMER2 web tool. Purity-adjusted Spearman's rank correlation test provided *P*-values and partial correlation (cor) values.

TYMS-related gene enrichment

The STRING website was employed to identify TYMS-binding proteins [32], with a low confidence score set at 0.7. Interaction types were based on the maximum number of interactors (≤50), full STRING network, and confidence.

Cell culture and transfection

We procured four cell lines, namely HeLa, A549, 786-O, and U87_MG, from Wuhan Pricella Biotechnology Co., Ltd. These cells were cultured at 37°C, 95% humidity, and 5% CO_2 in Dulbecco's Modified Eagle's Medium (DMEM) supplemented with 10% fetal bovine serum (FBS) sourced from Gibco, USA. The knockdown of TYMS in these cancer cell lines was achieved through the construction and transfection of siRNA-TYMS (siTYMS) and siRNA-NC (NC), serving as the corresponding control (obtained from Syngenbio, China). siTYMS sequence was 5' to 3' GCUACAGCCUGAGAGAUUATT/UAAUCUCUCAGGCUGUAGCTT. Upon reaching a cell density exceeding 80%, cells were seeded into 6-well plates, followed by transfection with siRNA-TYMS and siRNA-NC. The cells were then incubated in a stationary incubator. Transfection efficiency was evaluated by western blot analysis after 48 hours.

Western blot

Cellular proteins were extracted using RIPA lysate, and subsequently separated along with markers through electrophoresis utilizing SDS-PAGE gel (WSHT Biotechnology Inc., China), following the detailed method outlined in our previous article [33]. In brief, primary antibodies, including TYMS antibody (ab108995, Abcam, UK) and β-tubulin antibody (ab179513, Abcam, UK), were incubated overnight at 4°C. Following this, the membranes were subjected to three washes with TBST and then incubated with a secondary antibody for 1 hour at room temperature (Abcam, UK). The membranes were then analyzed for the expression of each group of protein bands using a ChemiDoc XRS machine (Bio-Rad, USA), and the results were analyzed using ImageJ (V 1.8.0).

Cell proliferation

The four types of transfected tumor cells were seeded into 96-well plates at a density of 2,000 cells per well. CellTiter-Glo assay (Promega, USA) was performed at 0, 24, 48, 72, and 96 hours after the cells had adhered to the wells. Luminescence (RLU) was measured using a microplate reader (TECAN Spark, Switzerland), and the results were analyzed for comparison between the NC and siTYMS groups.

Invasion

Transwell assays were performed to assess the impact of TYMS on the invasion of different cell types. Initially, the transwell inserts were coated with Matrigel (Corning Matrigel, USA) and incubated in a stationary incubator for 3 hours

to allow for solidification. Subsequently, 5×10^4 cells were seeded into the upper chamber of the transwell inserts, which were equipped with 8 μm wells and filled with serum-free DMEM. The lower chamber was filled with DMEM containing 10% FBS. After 24 hours of incubation, the cells at the bottom of the upper chamber were fixed, stained, and then captured for analysis.

Statistical analysis

The R software (Version 4.2.3) along with the "ggplot2" and "enrichplot" packages were employed for bioinformatic analysis. GraphPad Prism 7.0 was utilized to analyze biological data and generate graphical representations. All experiments were independently performed three times. Statistical differences between groups were calculated using the t-test or ANOVA as appropriate. Significance was defined as a *p*-value less than 0.05.

Data availability

The datasets analyzed in this study are available in the online dataset. Requests for further access to the dataset can be directed to yibo.geng@ccmu.edu.cn.

Results

Gene location and protein structure

We investigated the oncogenic function of TYMS which is located on 18p11.32 and gene length was 15,926 bp (NM_001071 or NP_001062.1, Supplementary Figure 1A). The protein structure of TYMS was conserved across various species (Supplementary Figure 1B, 1C).

Gene expression analysis

TYMS expression in multiple tumors, including bladder urothelial carcinoma (BLCA), BRCA, cervical squamous cell carcinoma and endocervical adenocarcinoma (CESC), cholangiocarcinoma (CHOL), COAD, esophageal carcinoma (ESCA), glioblastoma (GBM), head and neck squamous cell carcinoma (HNSC), kidney renal clear cell carcinoma (KIRC), kidney renal papillary cell carcinoma (KIRP), LIHC, LUAD, lung squamous cell carcinoma (LUSC), pheochromocytoma and paraganglioma (PCPG), stomach adenocarcinoma (STAD), thymoma (THYM), and uterine corpus endometrial carcinoma (UCEC), was higher than that in corresponding normal tissues (**Figure 2A**, P<0.01). Further analysis using the GTEx dataset revealed significant differences in expression levels between tumor and normal tissue in additional cancers (**Figure 2B**, P<0.05). However, TYMS expression in kidney chromophobe (KICH), prostatic adenocarcinoma (PRAD), testicular germ cell tumors (TGCT), or thyroid carcinoma (THCA) was similar to normal tissue (Supplementary Figure 2, P>0.05).

Positive correlations were found between TYMS expression and pathologic stage in adrenocortical carcinoma (ACC), KICH, LIHC, and TGCT. Conversely, COAD, LUSC, and ovarian serous cystadenocarcinoma (OV) showed negative correlations (**Figure 3**). No correlation was observed in other cancers (Supplementary Figure 3).

Immunohistochemical findings

Comparison of TYMS staining between normal and tumor tissues by IHC corroborated TYMS expression patterns in the HPA dataset. Medium or strong TYMS staining was observed in BRCA, COAD, LIHC, and LUAD, while low or negative staining was evident in normal comparable tissues (**Figure 4**).

Survival analysis

High TYMS expression correlated with poor overall survival in ACC (P<0.001, HR=3.8), KICH (P<0.05, HR=9.2), low grade glioma (LGG, P<0.001, HR=2.1), LIHC (P<0.001, HR=1.8), LUAD (P<0.001, HR=1.7), mesothelioma (MESO, P<0.001, HR=3.3) and sarcoma (SARC, P<0.01, HR=1.8) (**Figure 5A**). Similarly, it was associated with poor DFS in ACC (P<0.001, HR=4.9), KICH (P<0.05, HR=4.9), LGG (P<0.01, HR=1.5), LIHC (P<0.001, HR=1.8), PRAD (P<0.001, HR=2.0) and SARC (P<0.05, HR=1.5) (**Figure 5B**). While TYMS showed varied associations with outcome across different cancers, certain cancers, including ACC, KICH, LGG, LIHC, and SARC exhibited consistent tendencies in both OS and DFS (**Figure 5**).

Genetic alteration

A genetic alteration of TYMS has been observed in distinct tumors. The highest alteration frequency of TYMS (>4%) found in patients with

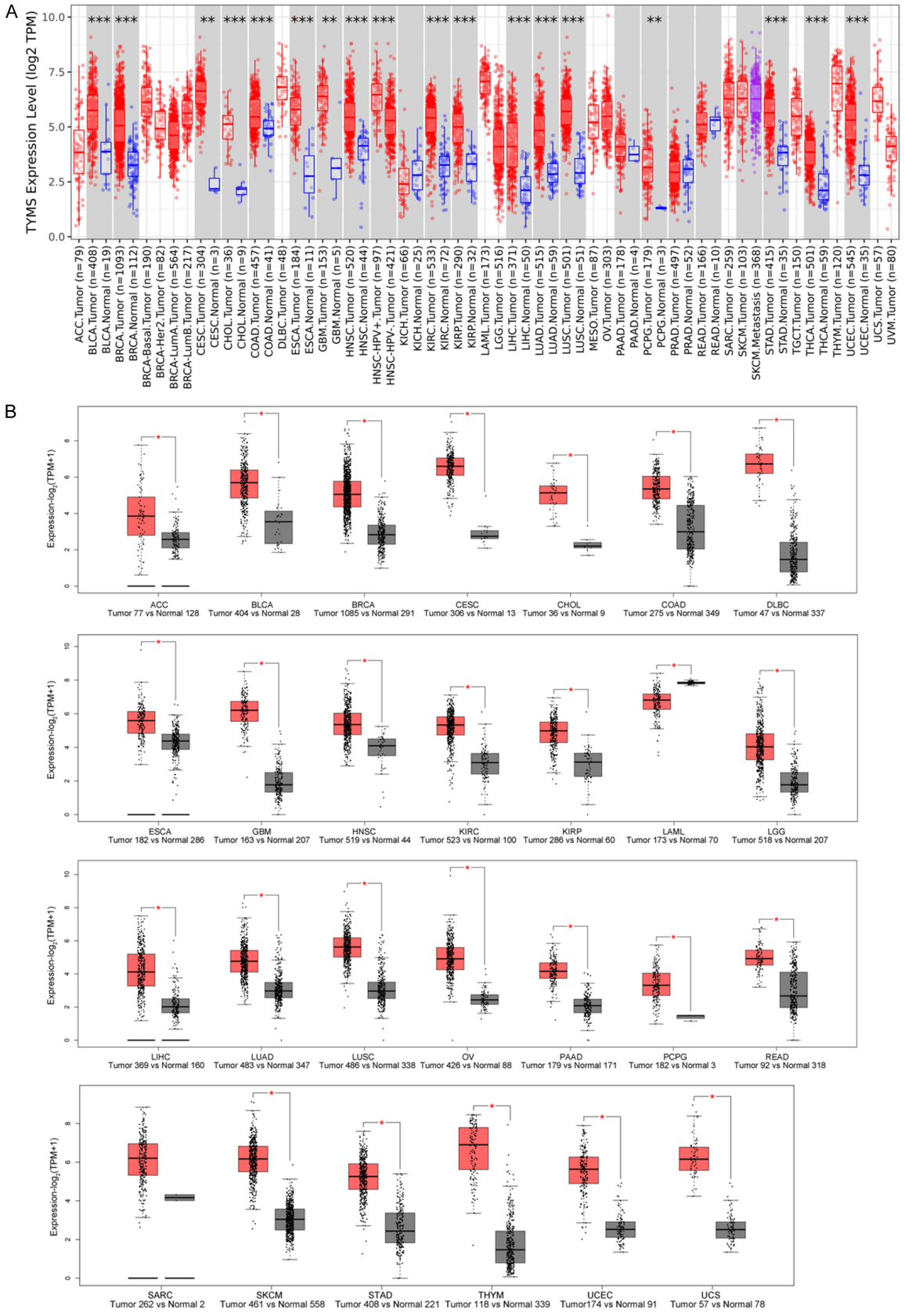

Figure 2. TYMS expression difference across various tumors. A. TYMS expression between various tumors and comparable normal tissues through TCGA dataset. B. TYMS expression through TCGA and GTEx dataset. *P<0.05; **P<0.01; ***P<0.001. TCGA, the Cancer Genome Atlas; GTEx, genotype-tissue expression.

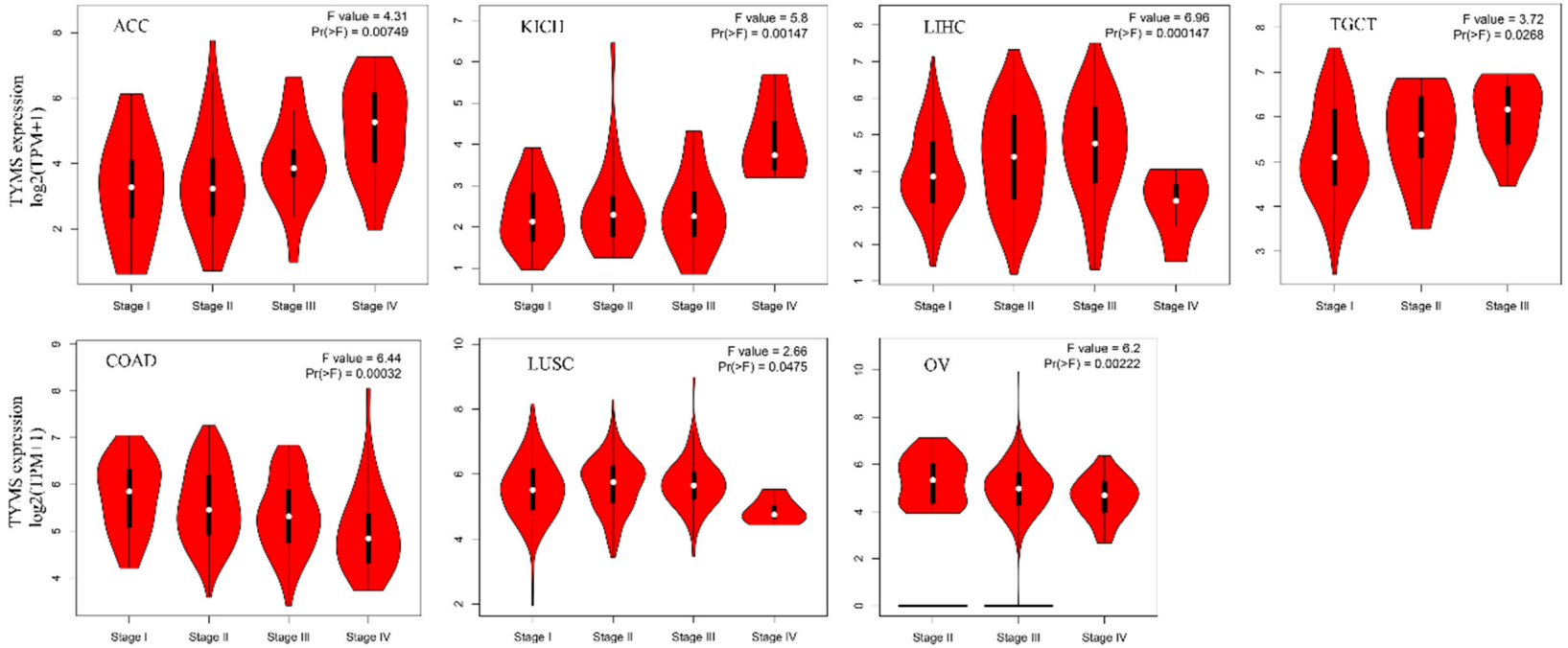

Figure 3. TYMS expression difference across pathological stages in seven tumor types.

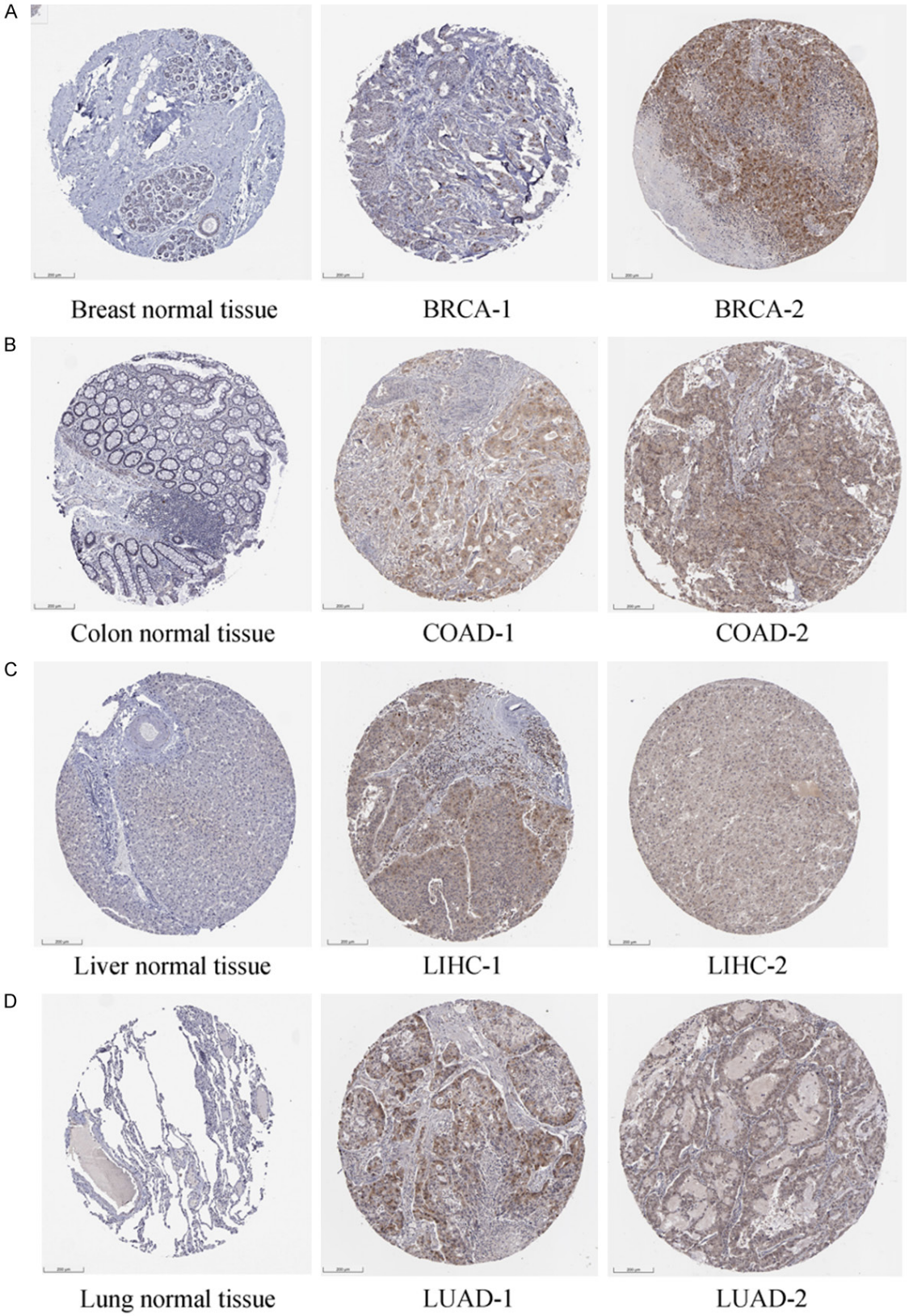

Figure 4. IHC difference between normal and tumor tissues in BRCA (A), COAD (B), LIHC (C) and LUAD (D). Negative or low IHC staining was obtained in the normal breast, colon, liver, and lung tissue, while medium or strong staining was obtained in the cancer tissue. IHC, immunohistochemistry; BRCA, breast invasive carcinoma; COAD, colon adenocarcinoma; LIHC, liver hepatocellular carcinoma; LUAD, lung adenocarcinoma. Scale bar: 200 um.

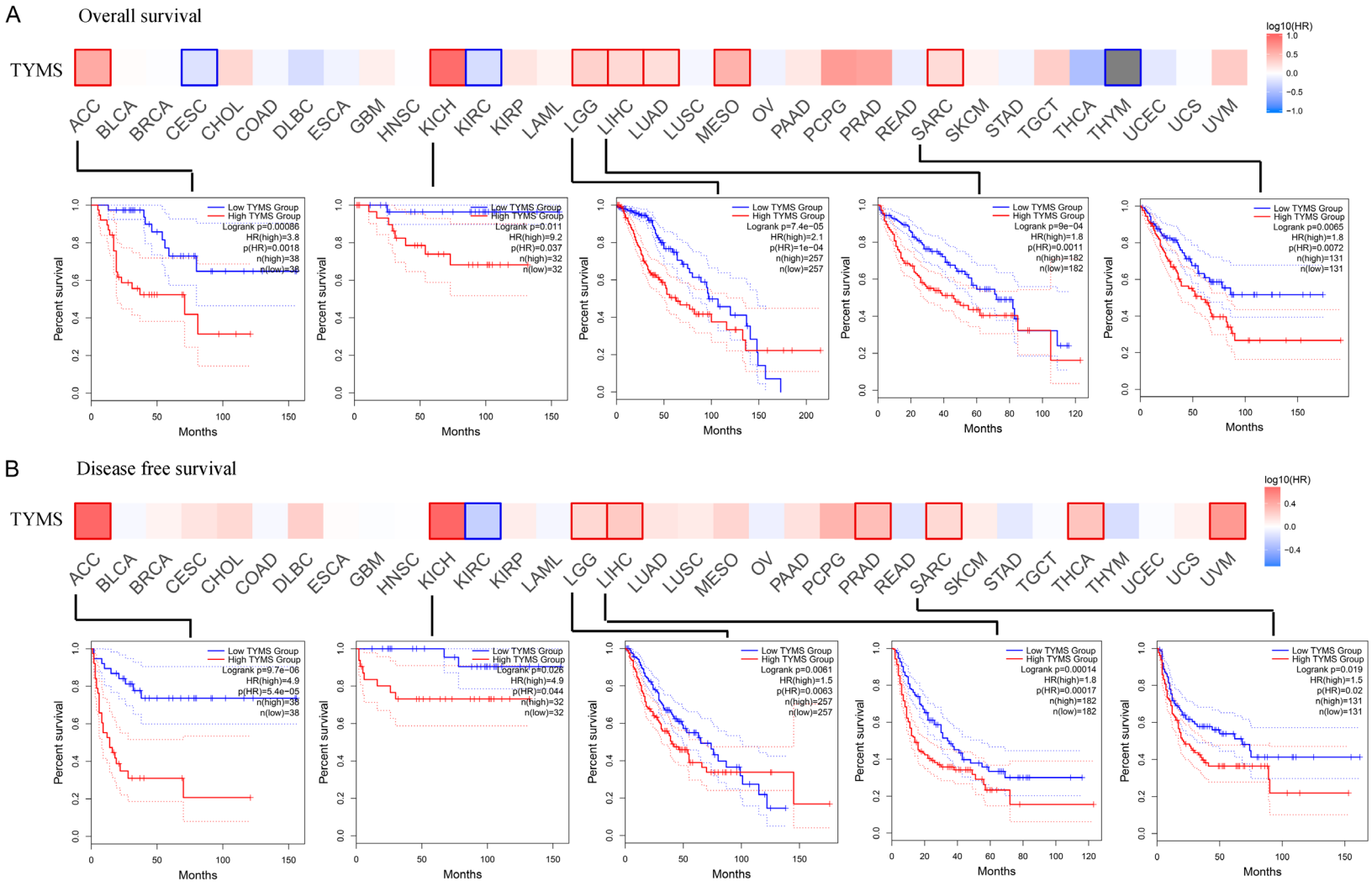

Figure 5. Correlation between TYMS expression and the survival outcome of tumors. OS (A) and DFS (B) are presented in the heat bar. A significantly similar trend was found between OS and DFS with ACC, KICH, LGG, LIHC and SARC, which is displayed in survival map (P<0.05). OS, overall survival; DFS, disease free survival; ACC, adrenocortical carcinoma; KICH, kidney chromophobe; LGG, low grade glioma; LIHC, liver hepatocellular carcinoma; SARC, sarcoma.

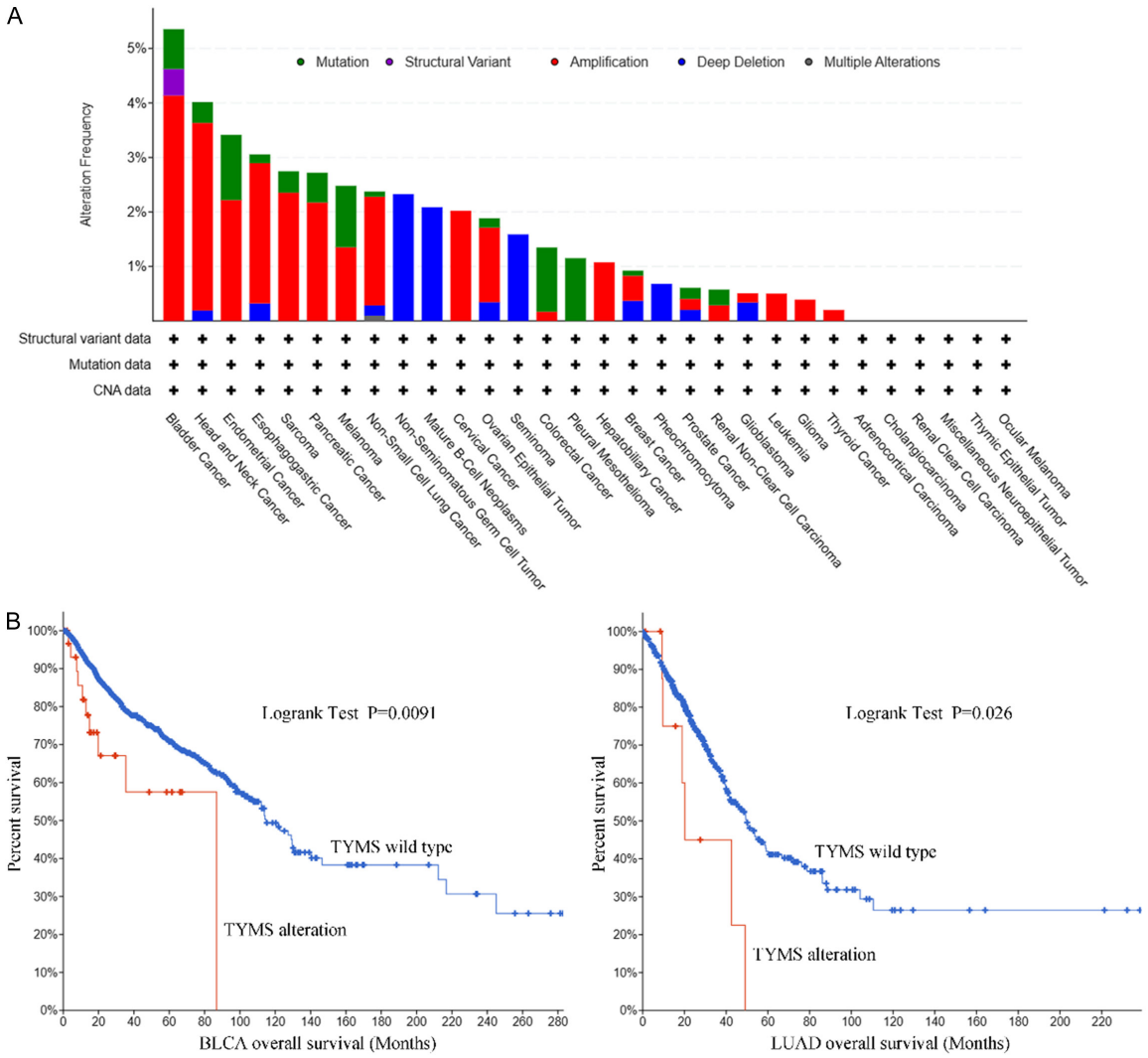

Figure 6. Mutation features of TYMS. A. The alteration frequency with mutation type is displayed. B. There are significant overall survival differences between TYMS alteration and wild-type in BLCA and LUAD (P<0.05). BLCA, bladder urothelial carcinoma; LUAD, lung adenocarcinoma.

bladder cancer was amplification (**Figure 6A**). Overall survival in the TYMS alteration group was significantly shorter than in the wild type for both BLCA (P<0.01) and LUAD (**Figure 6B**, P<0.05).

Phosphorylation analysis

Phosphorylation site analysis of TYMS in mammals was achieved using the PhosphoNET database (Supplementary Figure 4). Unfortunately, limited studies explored phosphorylation differences between tumor and normal tissues (Supplementary File 1), preventing a comprehensive summary of the implications of TYMS phosphorylation in tumors.

Immune infiltration analysis

Tumor-infiltrating immune cells can enhance the development, progression, or metastasis of cancers [34]. A significant negative relationship was found between CD4+ T cells and TYMS expression in BLCA, diffuse large B-cell lymphoma (DLBC), and MESO and the whole types of tumors showed positive correlation between CD4+Th2 cells and TYMS expression (**Figure 7A**, marked as vertical and horizontal red borders). Additionally, a significant relationship between TYMS expression and cancer-associated fibroblasts was observed for BRCA, HNSC, KICH, STAD, TGCT, and THYM. Among these, BRCA, HNSC, STAD, and THYM exhibited a neg-

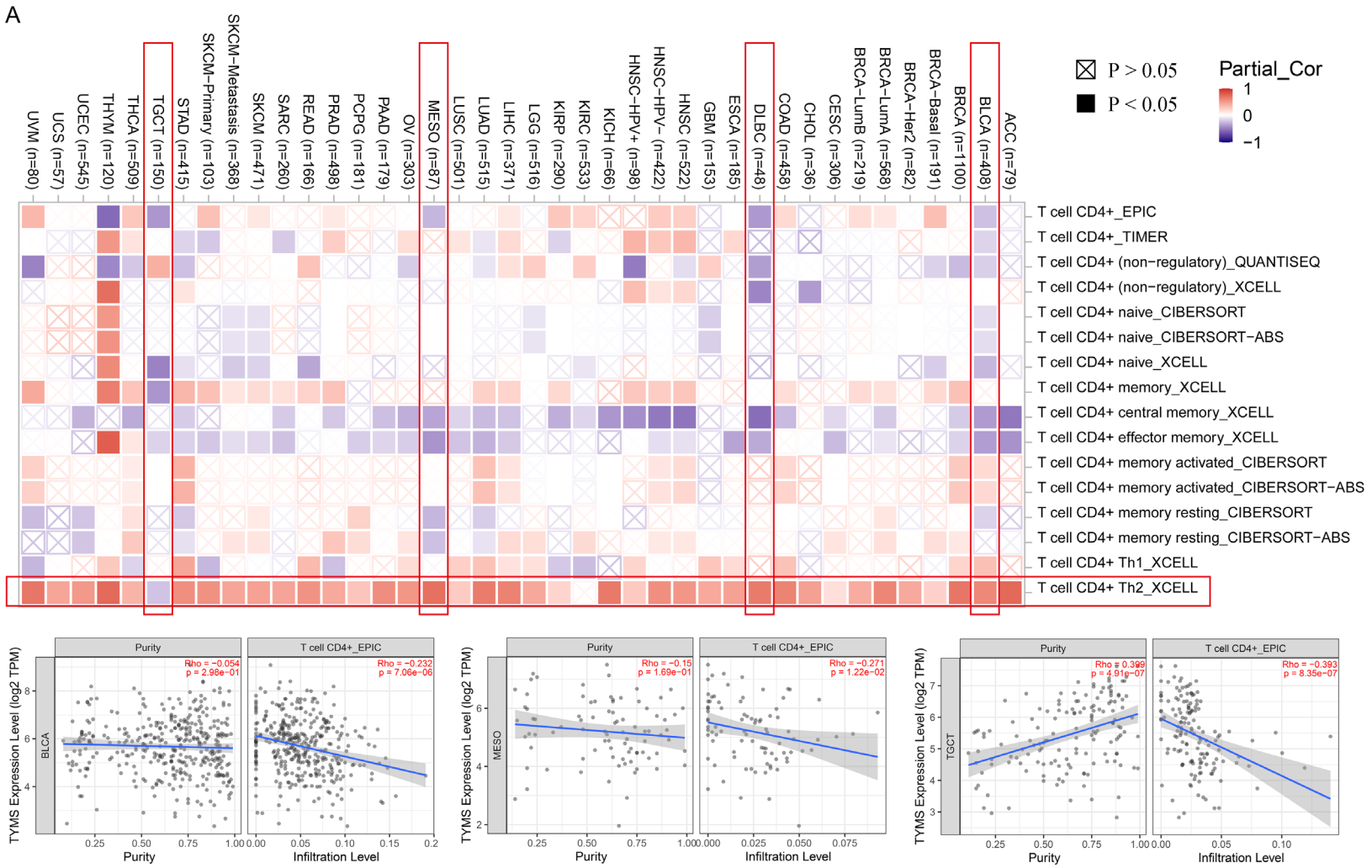
A
UVM (n=80)
UCS (n=57)
UCEC (n=545)
THYM (n=120)
THCA (n=509)
TGCT (n=150)
STAD (n=415)
SKCM−Primary (n=103)
SKCM−Metastasis (n=368)
SKCM (n=471)
SARC (n=260)
READ (n=166)
PRAD (n=498)
PCPG (n=181)
PAAD (n=179)
OV (n=303)
MESO (n=87)
LUSC (n=501)
LUAD (n=515)
LIHC (n=371)
LGG (n=516)
KIRP (n=290)
KIRC (n=533)
KICH (n=66)
HNSC−HPV+ (n=98)
HNSC−HPV− (n=422)
HNSC (n=522)
GBM (n=153)
ESCA (n=185)
DLBC (n=48)
COAD (n=458)
CHOL (n=36)
CESC (n=306)
BRCA−LumB (n=219)
BRCA−LumA (n=568)
BRCA−Her2 (n=82)
BRCA−Basal (n=191)
BRCA (n=1100)
BLCA (n=408)
ACC (n=79)
P > 0.05
P < 0.05
Partial_Cor
1
0
−1
T cell CD4+_EPIC
T cell CD4+_TIMER
T cell CD4+ (non−regulatory)_QUANTISEQ
T cell CD4+ (non−regulatory)_XCELL
T cell CD4+ naive_CIBERSORT
T cell CD4+ naive_CIBERSORT−ABS
T cell CD4+ naive_XCELL
T cell CD4+ memory_XCELL
T cell CD4+ central memory_XCELL
T cell CD4+ effector memory_XCELL
T cell CD4+ memory activated_CIBERSORT
T cell CD4+ memory activated_CIBERSORT−ABS
T cell CD4+ memory resting_CIBERSORT
T cell CD4+ memory resting_CIBERSORT−ABS
T cell CD4+ Th1_XCELL
T cell CD4+ Th2_XCELL
Purity
T cell CD4+_EPIC
Rho = −0.054
p = 2.98e−01
Rho = −0.232
p = 7.06e−06
TYMS Expression Level (log2 TPM)
BLCA
Purity
Infiltration Level
Rho = −0.15
p = 1.69e−01
Rho = −0.271
p = 1.22e−02
MESO
Rho = 0.399
p = 4.91e−07
Rho = −0.393
p = 8.35e−07
TGCT

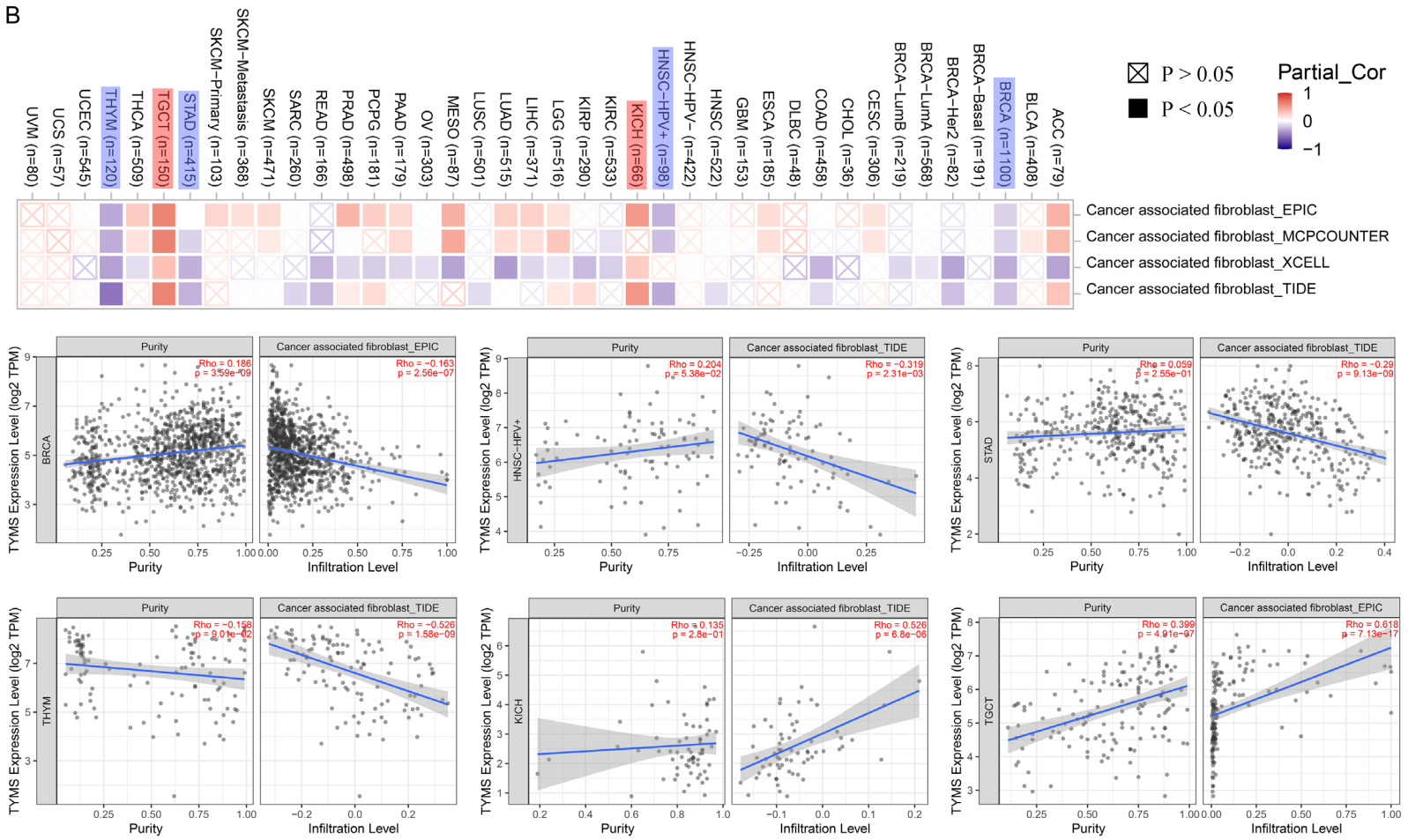

Figure 7. Correlation between TYMS and CD4+ immune cells (A) and cancer associated fibroblast (B).

ative correlation (**Figure 7B**). However, similar trends were not observed in CD8+ and NK cell types (Supplementary Figure 5).

Enrichment analysis of TYMS-related genes

Fifty TYMS-binding proteins were identified through the STRING tool (**Figure 8A**). The top 100 TYMS-correlated targeting genes were summarized, with the top five being NDC80, EZH2, NUSAP1, WDR76, and MCM6 (Supplementary Table 2). Notably, five genes overlapped in the two datasets (**Figure 8B**). The expression of these interacting genes (CDC45, MAD2L1, MCM5, NUSAP1, and PCAN) positively correlated with TYMS expression across almost all types of cancer (**Figure 8C**, **8D**).

Next, gene ontology (GO) analysis for these genes indicated their predominant location in the chromosomal region and execution of nucleotidase activity (**Figure 9**). Furthermore, these genes were enriched in DNA replication, chromosome segregation, and nuclear division.

TYMS promoted cell proliferation and invasion in multiple cancers

To further explore the oncogenic role of TYMS in human cancers, we utilized siRNA to reduce TYMS expression in four different types of human cancers, and the efficiency of knockdown was assessed by Western blot analysis. As depicted in **Figure 10A**, TYMS protein expression levels were markedly decreased in all tested cell lines (Hela, A549, 7860, and U87-MG) compared to control conditions.

Given that cell proliferation and invasion are two key characteristics of tumor oncogenic significance, we conducted experiments to assess these traits using CellTiter-Glo and transwell assays, respectively. The results revealed that reducing TYMS expression led to a notable decrease in tumor cell growth across cervical carcinoma, non-small cell lung carcinoma (NSCLC), GBM, and KIRC (**Figure 10B**). Furthermore, as shown in **Figure 10C**, TYMS knockdown significantly inhibited cell invasion in these tumors. Overall, the suppression of TYMS interfered with the malignant characteristics of human cancers.

Discussion

TYMS, a folate-dependent essential enzyme, plays a pivotal role in generating intracellular de novo deoxythymidine monophosphate (dTMP), critical for DNA synthesis and repair [35]. Its involvement extends beyond tumorigenesis, encompassing functions in coronary artery disease [36], virus replication, and congenital disorders [37, 38]. This diversity underscores the significance of TYMS in various pathologic contexts. The expanding literature linking TYMS to tumors prompted our comprehensive analysis to elucidate its oncogenic role in diverse cancer types.

The conservation of TYMS protein structure across species suggests shared vital physiologic mechanisms. Notably, TYMS expression was elevated in tumor tissues compared to their normal counterparts, which underscores the potential influence of TYMS in various cellular processes, including genomic instability [9], epithelial-mesenchymal transition, and chemotherapy metabolism [39, 40].

High TYMS expression consistently correlated with shorter overall survival and advanced tumor stage across multiple cancers. Recently, several studies have reported similar findings. Lai et al. suggested that the level of TYMS could serve as a predictive marker for longer overall survival in unresectable hepatocellular carcinoma patients [41]. Zhang et al. demonstrated that knockdown of TYMS reduced proliferation and invasion, and promoted apoptosis of liposarcoma through both bioinformatic and biological evidence [42]. This association could be attributed to TYMS's dual role: directly promoting tumor cell proliferation and inducing chemoresistance. Additionally, TYMS contributed to multiple drug resistance, affecting responses to 5-fluorouracil (5-FU) in COAD [40], temozolomide in glioma [43], and platinum in NSCLC [44]. This resistance is due to distinct pathways, including AMPK-mTOR for temozolomide resistance, polymorphism for fluorouracil resistance and nucleic acid-biosynthetic pathway for pemetrexed resistance [45]. However, contrasting observations were noted in the survival analysis between TYMS and CESC or KIRC. The following studies may explain these discrepancies. 1) Zheng et al. studied patients post-COVID-19 infection, where the pandemic might

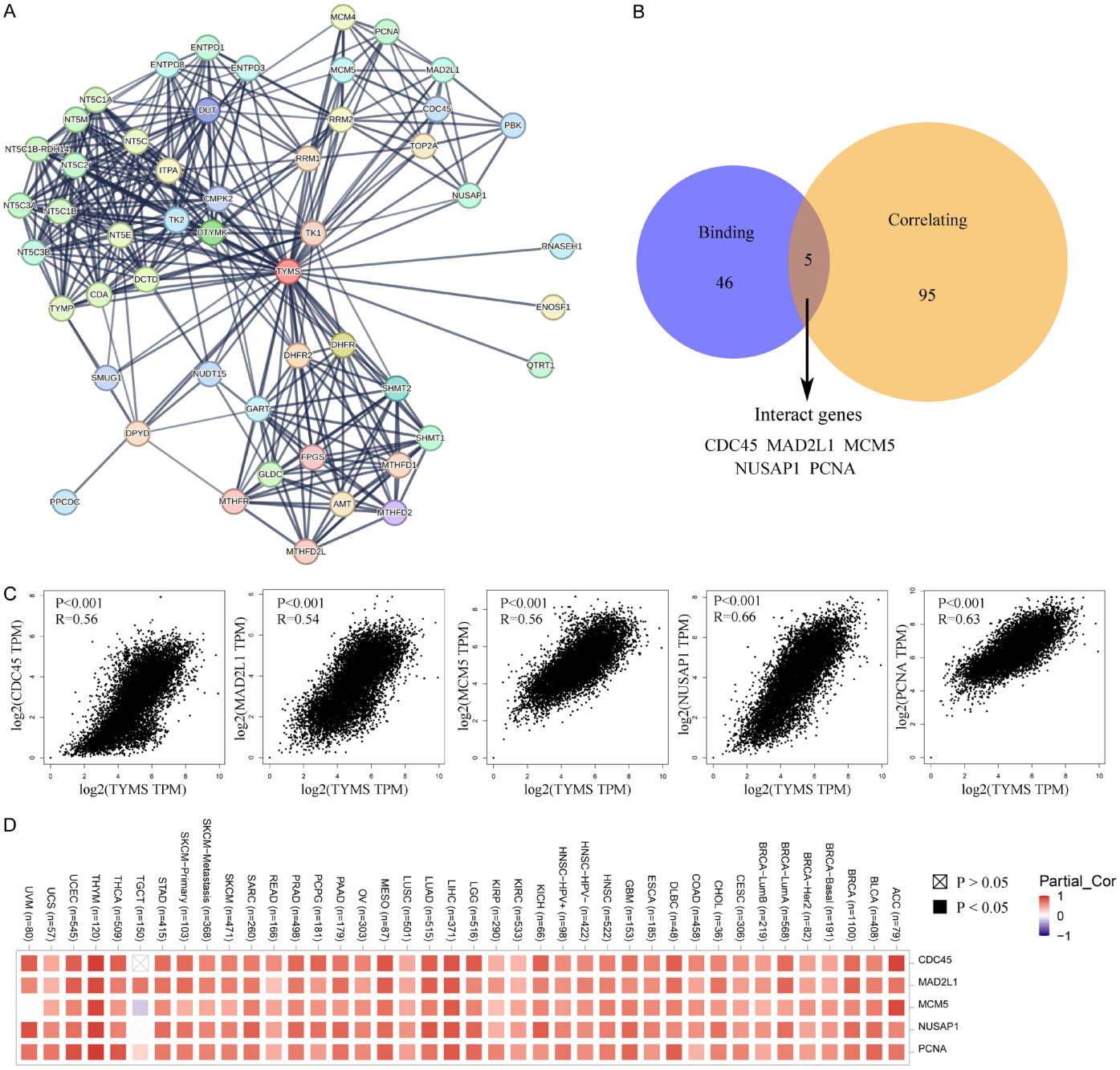
A
MCM4
PCNA
ENTPD1
ENTPD8
ENTPD3
MCM5
MAD2L1
NT5C1A
DUT
CDC45
NT5M
RRM2
PBK
NT5C1B-RDH14
NT5C
TOP2A
NT5C2
RRM1
ITPA
NUSAP1
NT5C3A
CMPK2
NT5C1B
TK2
DTYMK
TK1
NT5E
RNASEH1
NT5C3B
TYMS
DCTD
CDA
ENOSF1
TYMP
DHFR
DHFR2
QTRT1
SMUG1
NUDT15
SHMT2
GART
DPYD
SHMT1
FPGS
MTHFD1
GLDC
PPCDC
MTHFR
AMT
MTHFD2
MTHFD2L
B
Binding
46
5
Correlating
95
Interact genes
CDC45 MAD2L1 MCM5
NUSAP1 PCNA
C
P<0.001
R=0.56
log2(CDC45 TPM)
log2(TYMS TPM)
P<0.001
R=0.54
log2(MAD2L1 TPM)
log2(TYMS TPM)
P<0.001
R=0.56
log2(MCM5 TPM)
log2(TYMS TPM)
P<0.001
R=0.66
log2(NUSAP1 TPM)
log2(TYMS TPM)
P<0.001
R=0.63
log2(PCNA TPM)
log2(TYMS TPM)
D
UVM (n=80)
UCS (n=57)
UCEC (n=545)
THYM (n=120)
THCA (n=509)
TGCT (n=150)
STAD (n=415)
SKCM-Primary (n=103)
SKCM-Metastasis (n=368)
SKCM (n=471)
SARC (n=260)
READ (n=166)
PRAD (n=498)
PCPG (n=181)
PAAD (n=179)
OV (n=303)
MESO (n=87)
LUSC (n=501)
LUAD (n=515)
LIHC (n=371)
LGG (n=516)
KIRP (n=290)
KIRC (n=533)
KICH (n=66)
HNSC-HPV+ (n=98)
HNSC-HPV- (n=422)
HNSC (n=522)
GBM (n=153)
ESCA (n=185)
DLBC (n=48)
COAD (n=458)
CHOL (n=36)
CESC (n=306)
BRCA-LumB (n=219)
BRCA-LumA (n=568)
BRCA-Her2 (n=82)
BRCA-Basel (n=191)
BRCA (n=1100)
BLCA (n=408)
ACC (n=79)
P > 0.05
P < 0.05
Partial_Cor
1
0
−1
CDC45
MAD2L1
MCM5
NUSAP1
PCNA

Figure 8. TYMS-related gene analysis. (A) Top 50 TYMS-binding proteins and their relationship. (B) Degree of overlap between the TYMS-binding and correlated genes. (C) Expression analysis between TYMS and the five interacting genes in (B). (C, D) Displayed through heatmap across cancers.

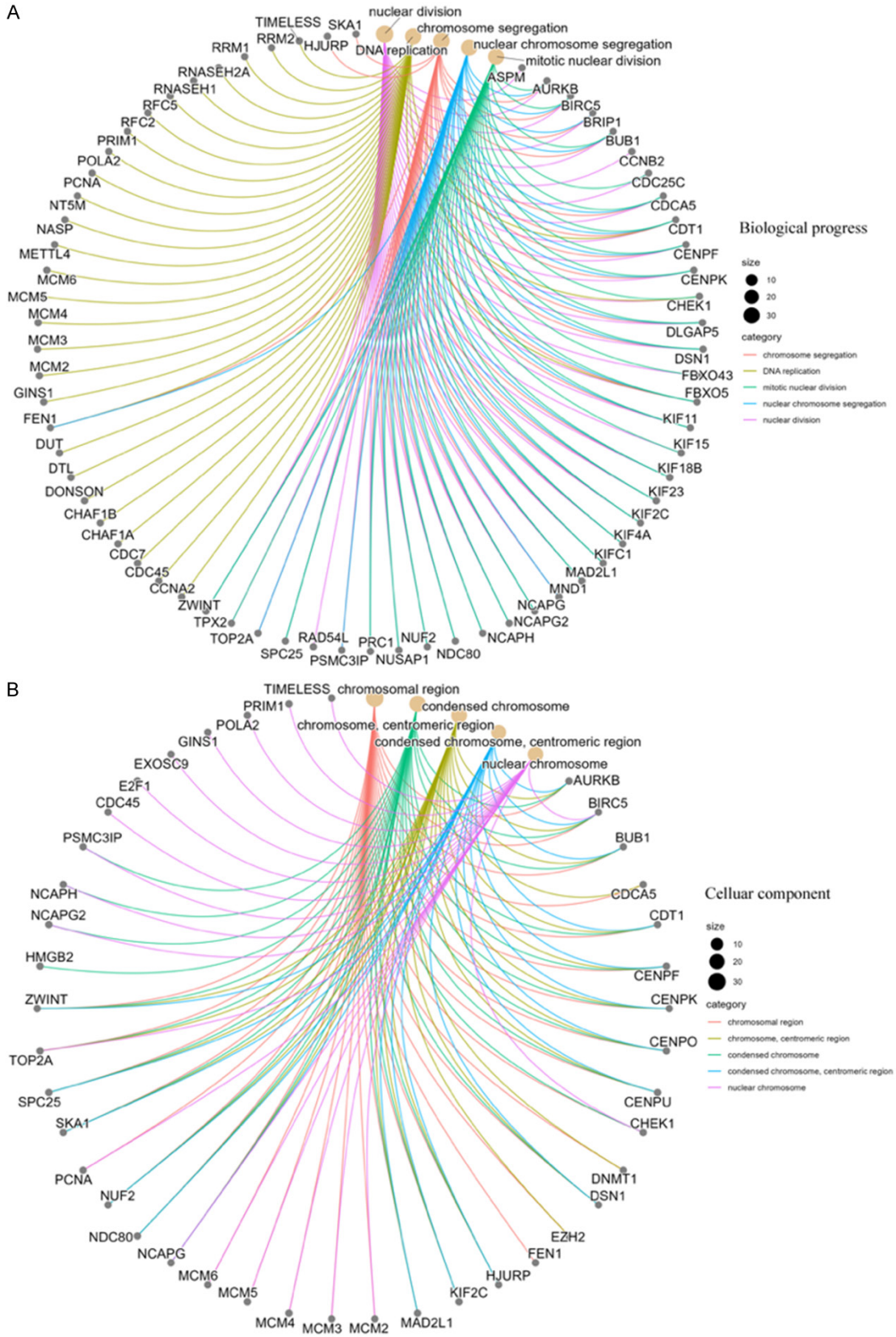

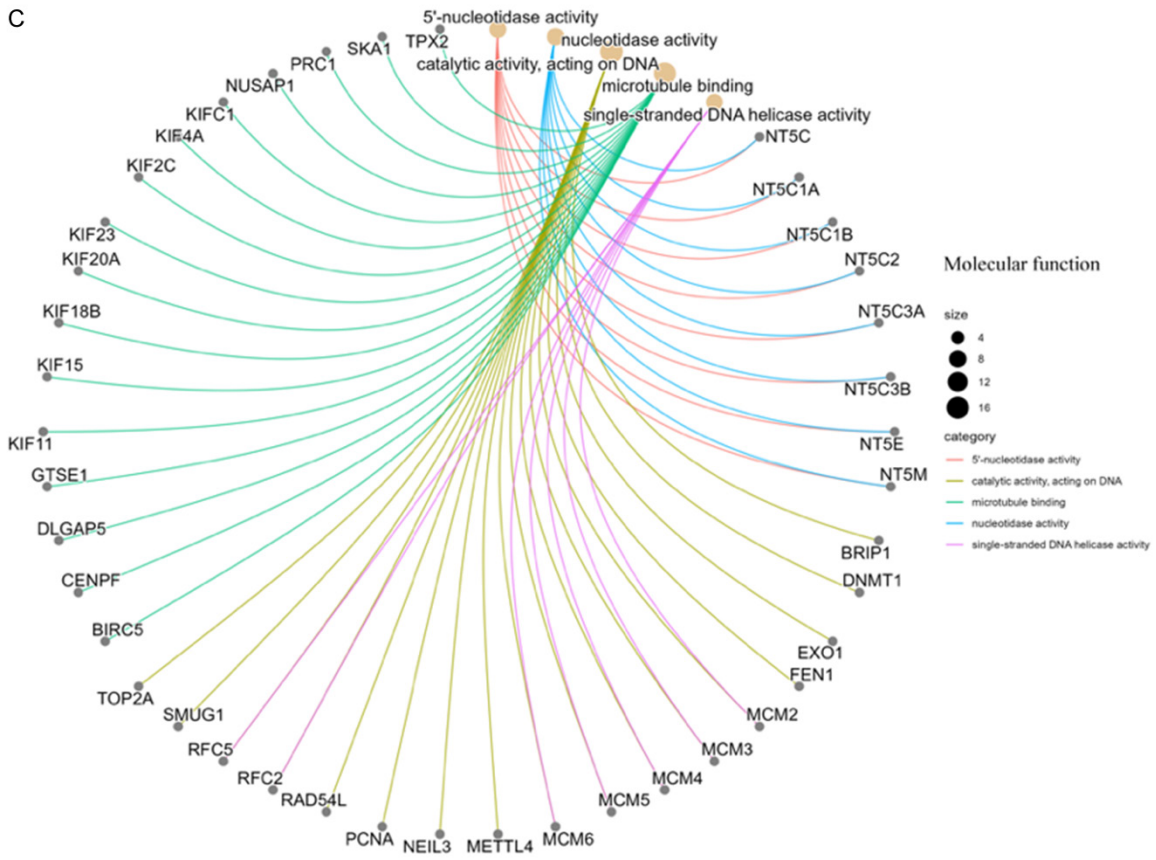

Figure 9. GO analysis of TYMS-related genes. Biological process (A), cellular components (B), and molecular function (C) are displayed. GO, gene ontology.

have altered the immune system and influenced TYMS expression [46]; 2) Fu et al. utilized four GEO datasets and the TCGA database, which might lead to different results compared to our single database analysis [47]. This suggests that TYMS may engage in divergent pathways across different tumor types.

The investigation into TYMS gene mutations and their functional implications remains an area requiring further exploration. To date, only a few studies have focused on this aspect. For instance, Shimizu et al. suggested that TYMS gene amplification could predict pemetrexed resistance in NSCLC [48]. Moreover, TYMS gene deletion has been associated with shorter overall survival in gastric cancer, possibly due to 5-FU chemoresistance [49]. In summary, several types of TYMS mutation have been noted to correlate with clinical characteristics. However, the underlying mechanisms behind these associations require further investigation.

The interaction between TYMS and tumor-infiltrating immune cells highlights its role in the tumor microenvironment. A significant difference was found between TYMS and CD4+ T-cells in BLCA, DLBC, MESO and TGCT (**Figure 7A**), which was similar with the previous studies. Dersh et al indicated that TYMS inhibitor increased major histocompatibility complex class I (MHC-1) presentation in DLBC, which revealed the role of TYMS in manipulating immunosurveillance in cancers [50]. Wang et al. demonstrated that TYMS suppression impaired helper T cells (Th1 & Th17) differentiation and immune response [51]. Above all, these results provide evidence that TYMS has a complicated correlation with immune system and deserves further studies in tumor immunology and microenvironment.

Enrichment analysis combining TYMS-binding components and expression-related genes revealed the central involvement of “nucleotidase activity” and “DNA replication” in tumor cell

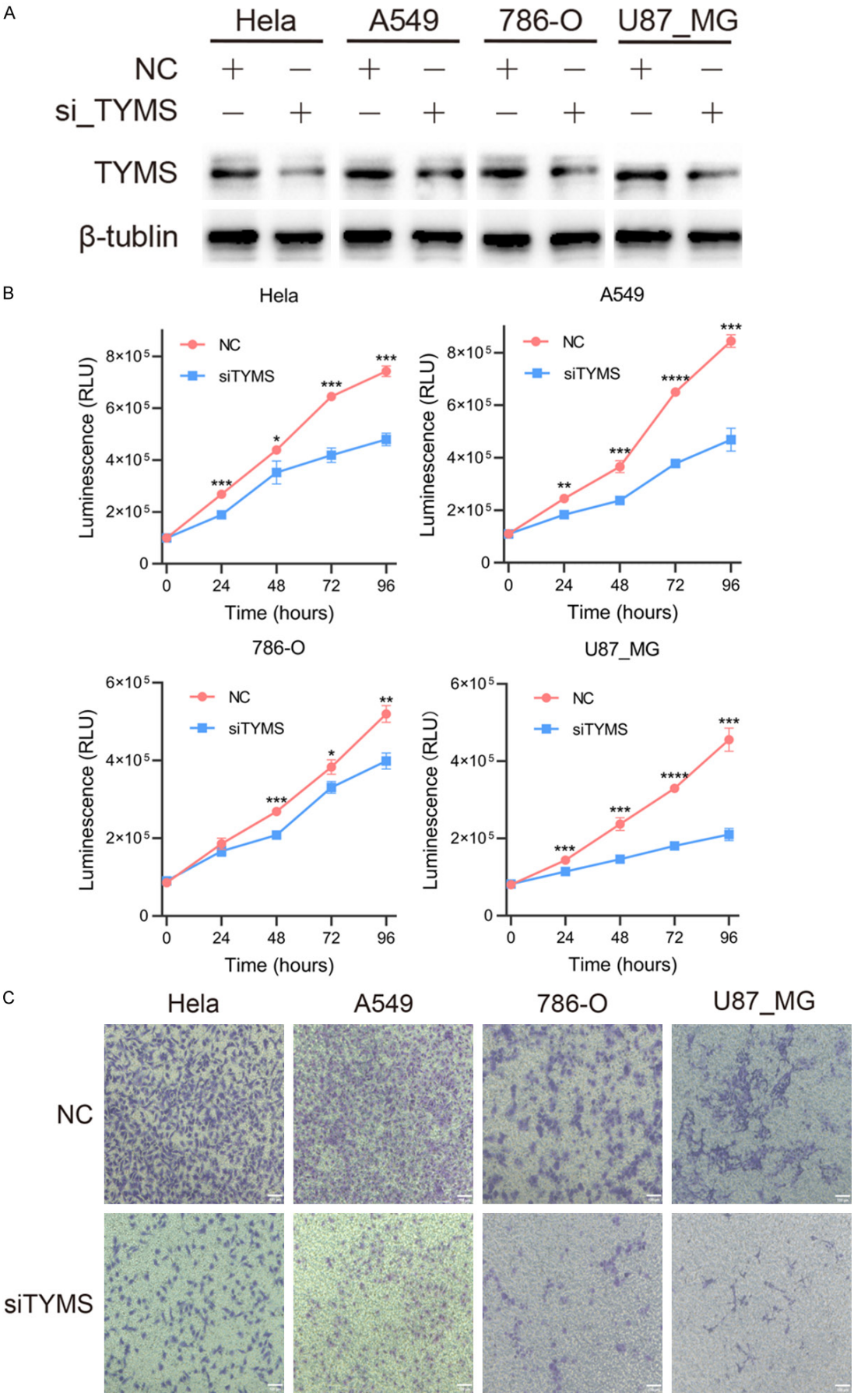
A
Hela
A549
786-O
U87_MG
NC
si_TYMS
TYMS
β-tublin
B
Hela
A549
786-O
U87_MG
NC
siTYMS
Luminescence (RLU)
Time (hours)
C
Hela
A549
786-O
U87_MG
NC
siTYMS

Figure 10. TYMS accelerated cell proliferation and migration of cervical carcinoma (Hela), NSCLC (A549), glioblastoma (U87_MG) and renal cell carcinoma (786-0). A. The protein expression levels of HeLa, A549, 786-0 and U87_MG cells after transfecting TYMS-specific siRNAs. B. Hela, A549, 786-0 and U87_MG cell growth was inhibited after TYMS knockdown. C. Migration of HeLa, A549, 786-0 and U87_MG cells were inhibited after transfecting TYMS-specific siRNAs (magnificance 100 μm) *P<0.05; **P<0.01; ***P<0.001; ****P<0.0001. NSCLC, non-small cell lung carcinoma; siRNA, small interfering RNA.

proliferation. These processes are pivotal in the progression of tumors, emphasizing the need for further experimental validation to elucidate the specific oncogenic role of TYMS. Future studies should delve into the molecular mechanisms underlying TYMS-mediated tumor progression and its use as a therapeutic target.

Finally, a series of cell experiments utilizing various tumor cell lines were conducted to validate the oncogenic function of TYMS identified through bioinformatic methods. Interestingly, while several studies employing the same cell lines have reported TYMS's oncogenic role, our results revealed an opposite trend. For instance, Fu et al. performed functional experiments and found that TYMS knockout could promote the proliferation, migration, and invasion of HeLa cells [47]. Conversely, Gotanda et al. demonstrated that TYMS decreased by miR-433 overexpression in HeLa cells resulted in inhibited cell proliferation [52], consistent with our findings. Notably, manipulation of TYMS expression in 786-0, U87_MG, or A549 cell lines has not been previously documented, suggesting significant gaps in TYMS research within the context of cancer. In our study, we found that suppression of TYMS also reversed the malignant characteristics of NSCLC, GBM and KIRC, a finding that has not been reported before. These findings underscore the complexity and variability of TYMS function across different tumor types and emphasize the need for further investigation in this field.

However, this study still presents several limitations that warrant improvement in future research endeavors. Firstly, our analysis of the oncogenic role was solely based on data derived from public databases, and thus, this conclusion needs to be validated in further clinical cohorts. Secondly, additional *in vitro* and *in vivo* experiments are necessary to elucidate the underlying mechanisms, particularly regarding the immune mechanisms involved. Thirdly, some of our results may be contradictory due to the inherent heterogeneity of data across multiple databases. These limitations underscore the need for continued research efforts to provide more comprehensive insight into the role of TYMS in cancer.

Conclusion

Based on a comprehensive analysis across various tumors, we found a factual association between TYMS expression and clinical outcome, protein phosphorylation and immune cell infiltration, as well as related genes and functions, which could help us understand the oncogenic role of TYMS.

Acknowledgements

This work was supported by the Beijing Municipal Natural Science Foundation (No. 7244344), Beijing Chaoyang Hospital Golden Seed foundation (No. CYJZ202201) and the inner-hospital foundation of Beijing Chaoyang Hospital. Besides, we would like to thank Xulei Huo for his technical supports.

Disclosure of conflict of interest

None.

Abbreviations

ACC, Adrenocortical carcinoma; BLCA, Bladder urothelial carcinoma; BRCA, Breast invasive carcinoma; CESC, Cervical squamous cell carcinoma and endocervical adenocarcinoma; CHOL, Cholangiocarcinoma; COAD, Colon adenocarcinoma; DFS, Disease free survival; DLBC, Diffuse large B-cell lymphoma; dTMP, deoxythymidine monophosphate; ESCA, Esophageal carcinoma; GBM, Glioblastoma; GEPIA2, Gene expression profiling interactive analysis, version 2; GO, Gene ontology; GTEx, Genotype-tissue expression; HNSC, Head and neck squamous cell carcinoma; HPA, The human protein atlas; IHC, Immunohistochemistry; KICH, Kidney chromophobe; KIRC, Kidney renal clear cell carcinoma; KIRP, Kidney renal papillary cell carcinoma; LAML, Acute myeloid leukemia; LGG, Low grade glioma; LIHC, Liver hepatocel-

lular carcinoma; LUAD, Lung adenocarcinoma; LUSC, Lung squamous cell carcinoma; MESO, Mesothelioma; MHC, Major histocompatibility complex; NCBI, National center for biotechnology information; NK, Natural killer; NSCLC, Non-small cell lung carcinoma; OS, Overall survival; OV, Ovarian serous cystadenocarcinoma; PAAD, Pancreatic adenocarcinoma; PCPG, Pheochromocytoma and paraganglioma; PRAD, Prostate adenocarcinoma; READ, Prostate adenocarcinoma; SARC, Sarcoma; SKCM, Skin cutaneous melanoma; STAD, Stomach adenocarcinoma; TCGA, The cancer genome atlas; TGCT, Testicular germ cell tumors; THCA, Thyroid carcinoma; THYM, Thymoma; TIMER2, Tumor immune estimation resource, version 2; TPM, Transcripts per million; TYMS, Thymidylate synthase; UCEC, Uterine corpus endometrial carcinoma; UCS, Uterine carcinosarcoma; UVM, Uveal melanoma.

Address correspondence to: Yan Wang, Department of Neurosurgery, Beijing Chaoyang Hospital, Capital Medical University, No. 8, South Road of Workers Stadium, Chaoyang District, Beijing 100020, China. E-mail: 13801110536@163.com; 122022010875@mail.ccmu.edu.cn

References

[1] Kontomanolis EN, Koutras A, Syllaios A, Schizas D, Mastoraki A, Garmpis N, Diakosavvas M, Angelou K, Tsatsaris G, Pagkalos A, Ntounis T and Fasoulakis Z. Role of oncogenes and tumor-suppressor genes in carcinogenesis: a review. Anticancer Res 2020; 40: 6009-6015.

[2] Blum A, Wang P and Zenklusen JC. SnapShot: TCGA-analyzed tumors. Cell 2018; 173: 530.

[3] Wang X, Guan Z, Dong Y, Zhu Z, Wang J and Niu B. Inhibition of thymidylate synthase affects neural tube development in mice. Reprod Toxicol 2018; 76: 17-25.

[4] Zhao Z, He S, Yu X, Lai X, Tang S, Mariya M EA, Wang M, Yan H, Huang X, Zeng S and Zha D. Analysis and experimental validation of rheumatoid arthritis innate immunity gene CYFIP2 and pan-cancer. Front Immunol 2022; 13: 954848.

[5] Meng Q, Li X and Xiong X. Identification of Hub genes associated with non-alcoholic steatohepatitis using integrated bioinformatics analysis. Front Genet 2022; 13: 872518.

[6] Lee HS, Chen M, Kim JH, Kim WH, Ahn S, Maeng K, Allegra CJ, Kaye FJ, Hochwald SN and Zajac-Kaye M. Analysis of 320 gastroenteropancreatic neuroendocrine tumors identifies TS expression as independent biomarker for survival. Int J Cancer 2014; 135: 128-137.

[7] Saviozzi S, Ceppi P, Novello S, Ghio P, Lo Iacono M, Borasio P, Cambieri A, Volante M, Papotti M, Calogero RA and Scagliotti GV. Non-small cell lung cancer exhibits transcript overexpression of genes associated with homologous recombination and DNA replication pathways. Cancer Res 2009; 69: 3390-3396.

[8] Wang L, Wu Z, Wang Y, Chen C, Li Y, Dong H, Yao T, Jin G and Wang Z. TYMS knockdown suppresses cells proliferation, promotes ferroptosis via inhibits PI3K/Akt/mTOR signaling pathway activation in triple negative breast cancer. Cell Biochem Biophys 2024; [Epub ahead of print].

[9] Guijarro MV, Nawab A, Dib P, Burkett S, Luo X, Feely M, Nasri E, Seifert RP, Kaye FJ and Zajac-Kaye M. TYMS promotes genomic instability and tumor progression in Ink4a/Arf null background. Oncogene 2023; 42: 1926-1939.

[10] Vijayakurup V, Maeng K, Lee HS, Meyer B, Burkett S, Nawab A, Dougherty MW, Jobin C, Mahmud I, Garrett TJ, Feely M, Lee KB, Kaye FJ, Guijarro MV and Zajac-Kaye M. Thymidylate synthase accelerates Men1-mediated pancreatic tumor progression and reduces survival. JCI Insight 2022; 7: e147417.

[11] Kumar A, Singh AK, Singh H, Thareja S and Kumar P. Regulation of thymidylate synthase: an approach to overcome 5-FU resistance in colorectal cancer. Med Oncol 2022; 40: 3.

[12] Costantino L, Ferrari S, Santucci M, Salo-Ahen OMH, Carosati E, Franchini S, Lauriola A, Pozzi C, Trande M, Gozzi G, Saxena P, Cannazza G, Losi L, Cardinale D, Venturelli A, Quotadamo A, Linciano P, Tagliazucchi L, Moschella MG, Guerrini R, Pacifico S, Luciani R, Genovese F, Henrich S, Alboni S, Santarem N, da Silva Cordeiro A, Giovannetti E, Peters GJ, Pinton P, Rimessi A, Cruciani G, Stroud RM, Wade RC, Mangani S, Marverti G, D'Arca D, Ponterini G and Costi MP. Destabilizers of the thymidylate synthase homodimer accelerate its proteasomal degradation and inhibit cancer growth. Elife 2022; 11: e73862.

[13] Banerjee S, Michalarea V, Ang JE, Ingles Garces A, Biondo A, Funingana IG, Little M, Ruddle R, Raynaud F, Riisnaes R, Gurel B, Chua S, Tunariu N, Porter JC, Prout T, Parmar M, Zachariou A, Turner A, Jenkins B, McIntosh S, Ainscow E, Minchom A, Lopez J, de Bono J, Jones R, Hall E, Cook N, Basu B and Banerji U. A Phase I trial of CT900, a novel alpha-folate receptor-mediated thymidylate synthase inhibitor, in patients with solid tumors with expansion cohorts in patients with high-grade serous ovarian cancer. Clin Cancer Res 2022; 28: 4634-4641.

[14] Siddiqui A, Gollavilli PN, Schwab A, Vazakidou ME, Ersan PG, Ramakrishnan M, Pluim D, Coggins S, Saatci O, Annaratone L, Hm

Schellens J, Kim B, Asangani IA, Rasheed SAK, Marchio C, Sahin O and Ceppi P. Thymidylate synthase maintains the de-differentiated state of triple negative breast cancers. Cell Death Differ 2019; 26: 2223-2236.

[15] Li B, Xu WW, Guan XY, Qin YR, Law S, Lee NP, Chan KT, Tam PY, Li YY, Chan KW, Yuen HF, Tsao SW, He QY and Cheung AL. Competitive binding between Id1 and E2F1 to Cdc20 regulates E2F1 degradation and thymidylate synthase expression to promote esophageal cancer chemoresistance. Clin Cancer Res 2016; 22: 1243-1255.

[16] Huang CL, Liu D, Nakano J, Yokomise H, Ueno M, Kadota K and Wada H. E2F1 overexpression correlates with thymidylate synthase and survivin gene expressions and tumor proliferation in non small-cell lung cancer. Clin Cancer Res 2007; 13: 6938-6946.

[17] Longley DB, Allen WL, McDermott U, Wilson TR, Latif T, Boyer J, Lynch M and Johnston PG. The roles of thymidylate synthase and p53 in regulating Fas-mediated apoptosis in response to antimetabolites. Clin Cancer Res 2004; 10: 3562-3571.

[18] Rahman L, Voeller D, Rahman M, Lipkowitz S, Allegra C, Barrett JC, Kaye FJ and Zajac-Kaye M. Thymidylate synthase as an oncogene: a novel role for an essential DNA synthesis enzyme. Cancer Cell 2004; 5: 341-351.

[19] Matuszyk J. MALAT1-miRNAs network regulate thymidylate synthase and affect 5FU-based chemotherapy. Mol Med 2022; 28: 89.

[20] Ciszewski WM, Chmielewska-Kassassir M, Wozniak LA and Sobierajska K. Thymidylate Synthase overexpression drives the invasive phenotype in colon cancer cells. Biomedicines 2022; 10: 1267.

[21] Nagaraju GP, Alese OB, Landry J, Diaz R and El-Rayes BF. HSP90 inhibition downregulates thymidylate synthase and sensitizes colorectal cancer cell lines to the effect of 5FU-based chemotherapy. Oncotarget 2014; 5: 9980-9991.

[22] Mannava S, Moparthy KC, Wheeler LJ, Leonova KI, Wawrzyniak JA, Bianchi-Smiraglia A, Berman AE, Flanagan S, Shewach DS, Zeitouni NC, Gudkov AV, Mathews CK and Nikiforov MA. Ribonucleotide reductase and thymidylate synthase or exogenous deoxyribonucleosides reduce DNA damage and senescence caused by C-MYC depletion. Aging (Albany NY) 2012; 4: 917-922.

[23] Fazzone W, Wilson PM, Labonte MJ, Lenz HJ and Ladner RD. Histone deacetylase inhibitors suppress thymidylate synthase gene expression and synergize with the fluoropyrimidines in colon cancer cells. Int J Cancer 2009; 125: 463-473.

[24] Sakatani A, Sonohara F and Goel A. Melatonin-mediated downregulation of thymidylate synthase as a novel mechanism for overcoming 5-fluorouracil associated chemoresistance in colorectal cancer cells. Carcinogenesis 2019; 40: 422-431.

[25] Li XY, Wang DP, Lu GQ, Liu KL, Zhang TJ, Li S, Mohamed O K, Xue WH, Qian XH and Meng FH. Development of a novel thymidylate synthase (TS) inhibitor capable of up-regulating P53 expression and inhibiting angiogenesis in NSCLC. J Adv Res 2020; 26: 95-110.

[26] Ko JC, Tsai MS, Chiu YF, Weng SH, Kuo YH and Lin YW. Up-regulation of extracellular signal-regulated kinase 1/2-dependent thymidylate synthase and thymidine phosphorylase contributes to cisplatin resistance in human non-small-cell lung cancer cells. J Pharmacol Exp Ther 2011; 338: 184-194.

[27] Kent WJ, Sugnet CW, Furey TS, Roskin KM, Pringle TH, Zahler AM and Haussler D. The human genome browser at UCSC. Genome Res 2002; 12: 996-1006.

[28] Gao J, Aksoy BA, Dogrusoz U, Dresdner G, Gross B, Sumer SO, Sun Y, Jacobsen A, Sinha R, Larsson E, Cerami E, Sander C and Schultz N. Integrative analysis of complex cancer genomics and clinical profiles using the cBioPortal. Sci Signal 2013; 6: pl1.

[29] Li T, Fu J, Zeng Z, Cohen D, Li J, Chen Q, Li B and Liu XS. TIMER2.0 for analysis of tumor-infiltrating immune cells. Nucleic Acids Res 2020; 48: W509-W514.

[30] Tang Z, Kang B, Li C, Chen T and Zhang Z. GEPIA2: an enhanced web server for large-scale expression profiling and interactive analysis. Nucleic Acids Res 2019; 47: W556-W560.

[31] Ponten F, Jirstrom K and Uhlen M. The human protein atlas--a tool for pathology. J Pathol 2008; 216: 387-393.

[32] Szklarczyk D, Gable AL, Lyon D, Junge A, Wyder S, Huerta-Cepas J, Simonovic M, Doncheva NT, Morris JH, Bork P, Jensen LJ and Mering CV. STRING v11: protein-protein association networks with increased coverage, supporting functional discovery in genome-wide experimental datasets. Nucleic Acids Res 2019; 47: D607-D613.

[33] Geng Y, Zuo P, Li XO and Zhang L. PODNL1 promotes cell proliferation and migration in glioma via regulating Akt/mTOR pathway. J Cancer 2020; 11: 6234-6242.

[34] Zhang Y and Zhang Z. The history and advances in cancer immunotherapy: understanding the characteristics of tumor-infiltrating immune cells and their therapeutic implications. Cell Mol Immunol 2020; 17: 807-821.

[35] Wilson PM, Danenberg PV, Johnston PG, Lenz HJ and Ladner RD. Standing the test of time:

targeting thymidylate biosynthesis in cancer therapy. Nat Rev Clin Oncol 2014; 11: 282-298.
[36] Kim JO, Ryu CS, Lee JY, Ko EJ, Ha YH, Sung JH, Hwang TS, Kim IJ and Kim NK. Association of thymidylate synthase (TS) gene polymorphisms with incidence and prognosis of coronary artery disease. Int J Mol Sci 2023; 24: 12591.
[37] Desrosiers V, Barat C, Breton Y, Ouellet M and Tremblay MJ. Thymidylate synthase is essential for efficient HIV-1 replication in macrophages. Virology 2021; 561: 47-57.
[38] Zhu H, Yang W, Shaw N, Perloff S, Carmichael SL, Finnell RH, Shaw GM and Lammer EJ. Thymidylate synthase polymorphisms and risk of conotruncal heart defects. Am J Med Genet A 2012; 158A: 2194-2203.
[39] Zhang F, Ye J, Guo W, Zhang F, Wang L and Han A. TYMS-TM4SF4 axis promotes the progression of colorectal cancer by EMT and upregulating stem cell marker. Am J Cancer Res 2022; 12: 1009-1026.
[40] Varghese V, Magnani L, Harada-Shoji N, Mauri F, Szydlo RM, Yao S, Lam EW and Kenny LM. FOXM1 modulates 5-FU resistance in colorectal cancer through regulating TYMS expression. Sci Rep 2019; 9: 1505.
[41] Lai Z, Huang Y, Wen D, Lin X, Kan A, Li Q, Wei W, Chen M, Xu L, He M and Shi M. One day versus two days of hepatic arterial infusion with oxaliplatin and fluorouracil for patients with unresectable hepatocellular carcinoma. BMC Med 2022; 20: 415.
[42] Zhang S, Yan L, Cui C, Wang Z, Wu J, Zhao M, Dong B, Guan X, Tian X and Hao C. Identification of TYMS as a promoting factor of retroperitoneal liposarcoma progression: Bioinformatics analysis and biological evidence. Oncol Rep 2020; 44: 565-576.
[43] Zhao M, Tan B, Dai X, Shao Y, He Q, Yang B, Wang J and Weng Q. DHFR/TYMS are positive regulators of glioma cell growth and modulate chemo-sensitivity to temozolomide. Eur J Pharmacol 2019; 863: 172665.
[44] Agullo-Ortuno MT, Garcia-Ruiz I, Diaz-Garcia CV, Enguita AB, Pardo-Marques V, Prieto-Garcia E, Ponce S, Iglesias L, Zugazagoitia J, Lopez-Martin JA, Paz-Ares L and Nunez JA. Blood mRNA expression of REV3L and TYMS as potential predictive biomarkers from platinum-based chemotherapy plus pemetrexed in non-small cell lung cancer patients. Cancer Chemother Pharmacol 2020; 85: 525-535.
[45] Sato Y, Tomita M, Soga T, Ochiai A and Makinoshima H. Upregulation of thymidylate synthase induces pemetrexed resistance in malignant pleural mesothelioma. Front Pharmacol 2021; 12: 718675.
[46] Zheng Z, Li X, Nie K, Wang X, Liang W, Yang F, Zheng K and Zheng Y. Identification of berberine as a potential therapeutic strategy for kidney clear cell carcinoma and COVID-19 based on analysis of large-scale datasets. Front Immunol 2023; 14: 1038651.
[47] Fu M, Pei Y, Lu F, Jiang H, Bi Y, Cheng J and Qin J. Identification of potential Hub genes and miRNA-mRNA pairs related to the progression and prognosis of cervical cancer through integrated bioinformatics analysis. Front Genet 2021; 12: 775006.
[48] Shimizu T, Nakagawa Y, Takahashi N and Hashimoto S. Thymidylate synthase gene amplification predicts pemetrexed resistance in patients with advanced non-small cell lung cancer. Clin Transl Oncol 2016; 18: 107-112.
[49] Biagioni A, Staderini F, Peri S, Versienti G, Schiavone N, Cianchi F, Papucci L and Magnelli L. 5-fluorouracil conversion pathway mutations in gastric cancer. Biology (Basel) 2020; 9: 265.
[50] Dersh D, Phelan JD, Gumina ME, Wang B, Arbuckle JH, Holly J, Kishton RJ, Markowitz TE, Seedhom MO, Fridlyand N, Wright GW, Huang DW, Ceribelli M, Thomas CJ, Lack JB, Restifo NP, Kristie TM, Staudt LM and Yewdell JW. Genome-wide screens identify lineage- and tumor-specific genes modulating MHC-I- and MHC-II-restricted immunosurveillance of human lymphomas. Immunity 2021; 54: 116-131, e110.
[51] Wang J, Peng L, Zhang R, Zheng Z, Chen C, Cheung KL, Cui M, Bian G, Xu F, Chiang D, Hu Y, Chen Y, Lu G, Yang J, Zhang H, Yang J, Zhu H, Chen SH, Liu K, Zhou MM, Sikora AG, Li L, Jiang B and Xiong H. 5-fluorouracil targets thymidylate synthase in the selective suppression of TH17 cell differentiation. Oncotarget 2016; 7: 19312-19326.
[52] Gotanda K, Hirota T, Matsumoto N and Ieiri I. MicroRNA-433 negatively regulates the expression of thymidylate synthase (TYMS) responsible for 5-fluorouracil sensitivity in HeLa cells. BMC Cancer 2013; 13: 369.

Supplementary File 1. The reference list related to TYMS phosphoprotein site in mammals.

[1] Very N, Hardivillé S, Decourcelle A, Thévenet J, Djouina M, Page A, Vergoten G, Schulz C, Kerr-Conte J, Lefebvre T, Dehennaut V and El Yazidi-Belkoura I. Thymidylate synthase O-GlcNAcylation: a molecular mechanism of 5-FU sensitization in colorectal cancer. Oncogene 2022; 41: 745-756.

[2] Akimov V, Barrio-Hernandez I, Hansen SVF, Hallenborg P, Pedersen AK, Bekker-Jensen DB, Puglia M, Christensen SDK, Vanselow JT, Nielsen MM, Kratchmarova I, Kelstrup CD, Olsen JV and Blagoev B. UbiSite approach for comprehensive mapping of lysine and N-terminal ubiquitination sites. Nat Struct Mol Biol 2018; 25: 631-640.

[3] Lumpkin RJ, Gu H, Zhu Y, Leonard M, Ahmad AS, Clauser KR, Meyer JG, Bennett EJ and Komives EA. Site-specific identification and quantitation of endogenous SUMO modifications under native conditions. Nat Commun 2017; 8: 1171.

[4] Mertins P, Mani DR, Ruggles KV, Gillette MA, Clauser KR, Wang P, Wang X, Qiao JW, Cao S, Petralia F, Kawaler E, Mundt F, Krug K, Tu Z, Lei JT, Gatza ML, Wilkerson M, Perou CM, Yellapantula V, Huang KL, Lin C, McLellan MD, Yan P, Davies SR, Townsend RR, Skates SJ, Wang J, Zhang B, Kinsinger CR, Mesri M, Rodriguez H, Ding L, Paulovich AG, Fenyö D, Ellis MJ and Carr SA; NCI CPTAC. Proteogenomics connects somatic mutations to signalling in breast cancer. Nature 2016; 534: 55-62.

[5] Boeing S, Williamson L, Encheva V, Gori I, Saunders RE, Instrell R, Aygün O, Rodriguez-Martinez M, Weems JC, Kelly GP, Conaway JW, Conaway RC, Stewart A, Howell M, Snijders AP and Svejstrup JQ. Multiomic analysis of the UV-Induced DNA damage response. Cell Rep 2016; 15: 1597-1610.

[6] Hendriks IA, D'Souza RC, Yang B, Verlaan-de Vries M, Mann M and Vertegaal AC. Uncovering global SUMOylation signaling networks in a site-specific manner. Nat Struct Mol Biol 2014; 21: 927-36.

[7] Mertins P, Yang F, Liu T, Mani DR, Petyuk VA, Gillette MA, Clauser KR, Qiao JW, Gritsenko MA, Moore RJ, Levine DA, Townsend R, Erdmann-Gilmore P, Snider JE, Davies SR, Ruggles KV, Fenyo D, Kitchens RT, Li S, Olvera N, Dao F, Rodriguez H, Chan DW, Liebler D, White F, Rodland KD, Mills GB, Smith RD, Paulovich AG, Ellis M and Carr SA. Ischemia in tumors induces early and sustained phosphorylation changes in stress kinase pathways but does not affect global protein levels. Mol Cell Proteomics 2014; 13: 1690-704.

[8] Tammsalu T, Matic I, Jaffray EG, Ibrahim AFM, Tatham MH and Hay RT. Proteome-wide identification of SUMO2 modification sites. Sci Signal 2014; 7: rs2.

[9] Mertins P, Qiao JW, Patel J, Udeshi ND, Clauser KR, Mani DR, Burgess MW, Gillette MA, Jaffe JD and Carr SA. Integrated proteomic analysis of post-translational modifications by serial enrichment. Nat Methods 2013; 10: 634-7.

[10] Udeshi ND, Svinkina T, Mertins P, Kuhn E, Mani DR, Qiao JW and Carr SA. Refined preparation and use of anti-diglycine remnant (K-ε-GG) antibody enables routine quantification of 10,000s of ubiquitination sites in single proteomics experiments. Mol Cell Proteomics 2013; 12: 825-31.

[11] Zhou H, Di Palma S, Preisinger C, Peng M, Polat AN, Heck AJ and Mohammed S. Toward a comprehensive characterization of a human cancer cell phosphoproteome. J Proteome Res 2013; 12: 260-71.

[12] Povlsen LK, Beli P, Wagner SA, Poulsen SL, Sylvestersen KB, Poulsen JW, Nielsen ML, Bekker-Jensen S, Mailand N and Choudhary C. Systems-wide analysis of ubiquitylation dynamics reveals a key role for PAF15 ubiquitylation in DNA-damage bypass. Nat Cell Biol 2012; 14: 1089-98.

[13] Klammer M, Kaminski M, Zedler A, Oppermann F, Blencke S, Marx S, Müller S, Tebbe A, Godl K and Schaab C. Phosphosignature predicts dasatinib response in non-small cell lung cancer. Mol Cell Proteomics 2012; 11: 651-68.

[14] Franz-Wachtel M, Eisler SA, Krug K, Wahl S, Carpy A, Nordheim A, Pfizenmaier K, Hausser A and Macek B. Global detection of protein kinase D-dependent phosphorylation events in nocodazole-treated human cells. Mol Cell Proteomics 2012; 11: 160-70.

[15] Beli P, Lukashchuk N, Wagner SA, Weinert BT, Olsen JV, Baskcomb L, Mann M, Jackson SP and Choudhary C. Proteomic investigations reveal a role for RNA processing factor THRAP3 in the DNA damage response. Mol Cell 2012; 46: 212-25.

[16] Weber C, Schreiber TB and Daub H. Dual phosphoproteomics and chemical proteomics analysis of erlotinib and gefitinib interference in acute myeloid leukemia cells. J Proteomics 2012; 75: 1343-56.

[17] Kim W, Bennett EJ, Huttlin EL, Guo A, Li J, Possemato A, Sowa ME, Rad R, Rush J, Comb MJ, Harper JW and Gygi SP. Systematic and quantitative assessment of the ubiquitin-modified proteome. Mol Cell 2011; 44: 325-40.

[18] Wagner SA, Beli P, Weinert BT, Nielsen ML, Cox J, Mann M and Choudhary C. A Proteome-wide, Quantitative survey of in vivo ubiquitylation sites reveals widespread regulatory roles. Mol Cell Proteomics 2011; 10: M111.013284.

[19] Kettenbach AN, Schweppe DK, Faherty BK, Pechenick D, Pletnev AA and Gerber SA. Quantitative phosphoproteomics identifies substrates and functional modules of aurora and polo-like kinase activities in mitotic cells. Sci Signal 2011; 4: rs5.
[20] Iliuk AB, Martin VA, Alicie BM, Geahlen RL and Tao WA. In-depth analyses of kinase-dependent tyrosine phosphoproteomes based on metal ion-functionalized soluble nanopolymers. Mol Cell Proteomics 2010; 9: 2162-72.
[21] Frączyk T, Kubiński K, Masłyk M, Cieśla J, Hellman U, Shugar D and Rode W. Phosphorylation of thymidylate synthase from various sources by human protein kinase CK2 and its catalytic subunits. Bioorg Chem 2010; 38: 124-131.
[22] Jarmuła A, Fraczyk T, Cieplak P and Rode W. Mechanism of influence of phosphorylation on serine 124 on a decrease of catalytic activity of human thymidylate synthase. Bioorg Med Chem 2010; 18: 3361-70.
[23] Olsen JV, Vermeulen M, Santamaria A, Kumar C, Miller ML, Jensen LJ, Gnad F, Cox J, Jensen TS, Nigg EA, Brunak S and Mann M. Quantitative phosphoproteomics reveals widespread full phosphorylation site occupancy during mitosis. Sci Signal 2010; 3: ra3.
[24] Jørgensen C, Sherman A, Chen GI, Pasculescu A, Poliakov A, Hsiung M, Larsen B, Wilkinson DG, Linding R and Pawson T. Cell-specific information processing in segregating populations of Eph receptor ephrin-expressing cells. Science 2009; 326: 1502-9.
[25] Choudhary C, Olsen JV, Brandts C, Cox J, Reddy PN, Böhmer FD, Gerke V, Schmidt-Arras DE, Berdel WE, Müller-Tidow C, Mann M and Serve H. Mislocalized activation of oncogenic RTKs switches downstream signaling outcomes. Mol Cell 2009; 36: 326-39.
[26] Mayya V, Lundgren DH, Hwang SI, Rezaul K, Wu L, Eng JK, Rodionov V and Han DK. Quantitative phosphoproteomic analysis of T cell receptor signaling reveals system-wide modulation of protein-protein interactions. Sci Signal 2009; 2: ra46.
[27] Anderson DD, Woeller CF and Stover PJ. Small ubiquitin-like modifier-1 (SUMO-1) modification of thymidylate synthase and dihydrofolate reductase. Clin Chem Lab Med 2007; 45: 1760-3.
[28] Rush J, Moritz A, Lee KA, Guo A, Goss VL, Spek EJ, Zhang H, Zha XM, Polakiewicz RD and Comb MJ. Immunoaffinity profiling of tyrosine phosphorylation in cancer cells. Nat Biotechnol 2005; 23: 94-101.

Supplementary Table 1. The detailed analysis of **Figure 1**

Ref. No.	Year	Journal	Summary
10	2022	JCI Insight	In Men1-mutant in vivo and in vitro background, increased levels of TYMS accelerate pancreatic neuroendocrine tumor cell proliferation, disrupt cell cycle regulation, and correlate with elevated somatic mutations, DNA damage, and genomic instability.
11	2022	Med Oncol	5-FU leads to resistance against TYMS targeting drugs. Various chemoresistance mechanisms include autophagy, apoptosis evasion, drug detoxification and altered signaling pathways containing AKT/PI3K, RAS-MAPK, WNT/β catenin, mTOR.
12	2022	Elife	E7, a novel anticancer drug, inhibits TYMS expression in both pancreatic and ovarian cancer cells and hastens its proteasomal degradation, lowering enzyme levels.
13	2022	Clin Cancer Res	Phase I clinical trials revealed CT900, a novel TYMS inhibitor targeting α-folate receptor, demonstrated an acceptable side effect profile and clinical benefit in patients with ovarian cancers.
14	2019	Cell Death Differ	In vitro, knockdown of TYMS attenuated migration and sphere formation while repressing the expression of epithelial-mesenchymal transition (EMT) signature genes. In vivo, cells deficient in TYMS demonstrated an increased ability to invade and metastasize. Mechanistically, TYMS enzymatic activity was found to be essential for maintaining the EMT/stem-like state by facilitating dihydropyrimidine dehydrogenase-dependent pyrimidine catabolism.
15	2016	Clin Cancer Res	Id1 was found to confer 5-FU chemoresistance through E2F1-dependent induction of TYMS expression in esophageal cancer. Additionally, an intricate E2F1-dependent mechanism was elucidated, whereby Id1 increases TYMS and IGF2 expressions to promote cancer chemoresistance.
16	2007	Clin Cancer Res	In NSCLC patiens, E2F1 gene expression correlates with TS gene expressions and tumor proliferation.
17	2004	Clin Cancer Res	The induction of TYMS expression inhibits Fas induction in response to raltitrexed and Alimta, leading to the inactivation of Caspase-8.
18	2004	Cancer Cell	Overexpression of TYMS results in programmed cell death following serum removal. The ectopic expression of TYMS is sufficient to induce a transformed phenotype in mammalian cells, as evidenced by foci formation, anchorage-independent growth, and tumor formation in nude mice.
19	2022	Mol Med	The MALAT1 lncRNA and miRNA (miR-197-3p, miR-203a-3p, miR-375-3p) network regulates TYMS expression and predicts chemoresistance to 5-FU treatment.
20	2022	Biomedicines	TYMS is involved in the modulation of epithelial-mesenchymal transition (EMT) and colorectal cancer metastasis. Silencing TYMS expression reverses EMT and inhibits the invasive capacity of cancer cells.
21	2014	Oncotarget	HSP90 knockdown inhibits cell cycle progression, downregulates TYMS levels, and sensitizes colorectal cancer cell lines to the effects of 5-FU.
22	2012	Aging	Simultaneous genetic inhibition of TYMS and ribonucleotide reductase in melanoma cells induces DNA damage and senescence phenotypes. Conversely, overexpression of TYMS and ribonucleotide reductase inhibits DNA damage and senescence-associated phenotypes caused by C-myc depletion.
23	2009	Int J Cancer	Histone deacetylase inhibitors (HDACi) significantly downregulate TYMS gene expression in colon cancer cell lines. This downregulation is independent of p53, p21, and HDAC2 expression and can be achieved in vivo, thereby contributing to overcoming chemoresistance to 5-FU.
24	2019	Carcino-genesis	Melatonin-mediated downregulation of thymidylate synthase as a novel mechanism for overcoming 5-fluorouracil associated chemoresistance in colorectal cancer cells.
25	2020	J Adv Res	A novel TYMS inhibitor induces apoptosis through the mitochondrial pathway in NSCLC cells by upregulating wild-type p53 protein expression. This compound also inhibits angiogenesis both in vitro and in vivo.
26	2011	J Pharmacol Exp Ther	Cisplatin increases the phosphorylation of mitogen-activated protein kinase kinase 1/2 (MKK1/2) and extracellular signal-regulated kinase 1/2 (ERK1/2), as well as the protein levels of TYMS, by enhancing protein stability in NSCLC cells. Depletion of endogenous TYMS expression significantly increases cisplatin-induced cell death and growth inhibition. Enforced expression of constitutively active MKK1/2 vectors rescues the protein levels of phospho-ERK1/2 and TYMS. In conclusion, the upregulation of ERK1/2-dependent TYMS protects NSCLC cells from cisplatin-induced cytotoxicity.

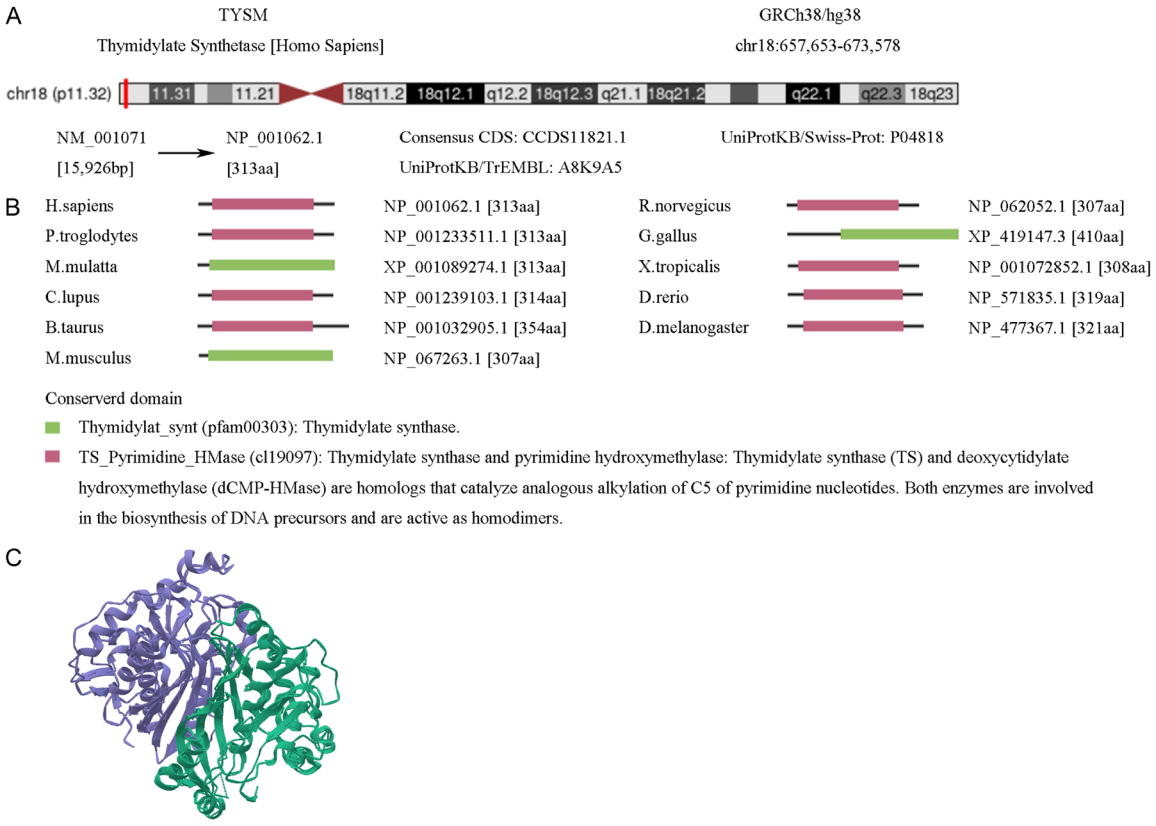

Supplementary Figure 1. Structural characteristics of TYMS. A. Gene location of TYMS. B. Conserved domain of TYMS. C. Three-dimension structure of TYMS.

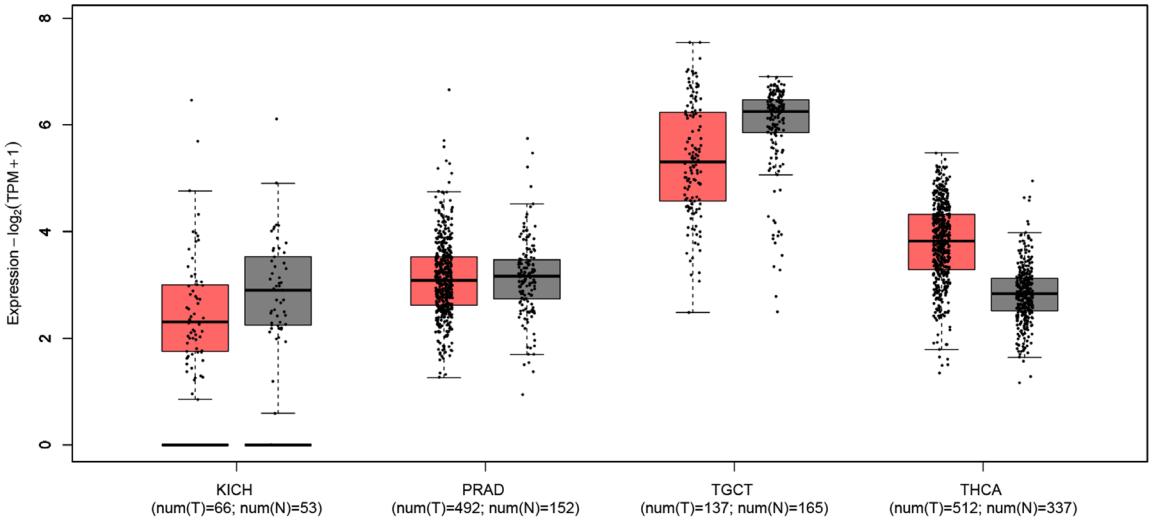

Supplementary Figure 2. TYMS expression showed no difference between KICH, PRAD, TGCT, or THCA and their comparable normal tissues. KICH, kidney chromophobe; PRAD, prostatic adenocarcinoma; TGCT, testicular germ cell tumors; THCA, thyroid carcinoma.

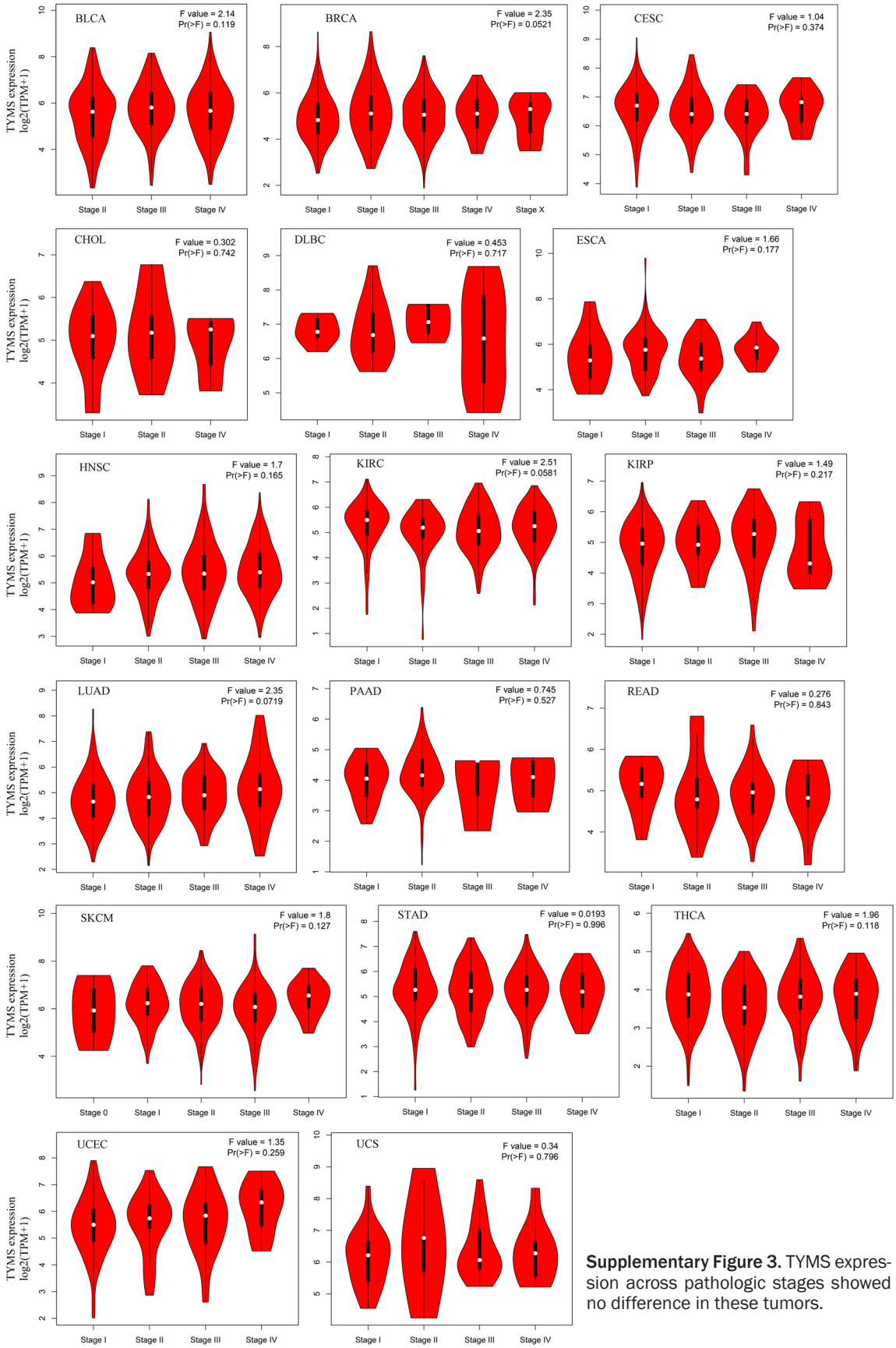

Supplementary Figure 3. TYMS expression across pathologic stages showed no difference in these tumors.

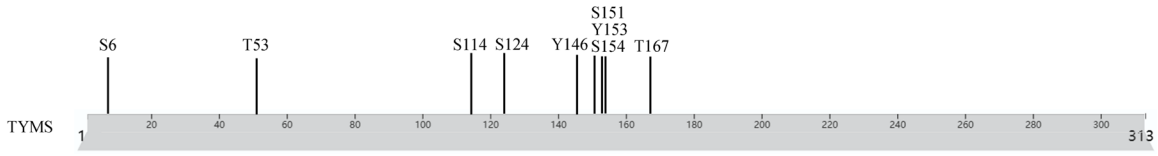

Supplementary Figure 4. Phosphoprotein site of TYMS showed in the axis.

Supplementary Figure 5. Correlation between TYMS and CD8+ immune cells (A) and NK cells (B). NK, natural killer.

Supplementary Table 2. Top 100 TYMS-correlated genes

Gene Symbol	Gene ID	Pearson correlation coefficient
NDC80	ENSG00000080986.12	0.73
EZH2	ENSG00000106462.10	0.66
NUSAP1	ENSG00000137804.12	0.66
WDR76	ENSG00000092470.11	0.65
MCM6	ENSG00000076003.4	0.65
KIFC1	ENSG00000237649.7	0.65
NCAPG	ENSG00000109805.9	0.64
KIF15	ENSG00000163808.16	0.64
LMNB1	ENSG00000113368.11	0.63
HMGB2	ENSG00000164104.11	0.63
FEN1	ENSG00000168496.3	0.63
PCNA	ENSG00000132646.10	0.63
GTSE1	ENSG00000075218.18	0.62
KIF2C	ENSG00000142945.12	0.62
MCM3	ENSG00000112118.17	0.61
PLK4	ENSG00000142731.10	0.61
CHAF1A	ENSG00000167670.15	0.61
CDC7	ENSG00000097046.12	0.61
CLSPN	ENSG00000092853.13	0.61
KIAA0101	ENSG00000166803.10	0.6
AURKB	ENSG00000178999.12	0.6
FANCI	ENSG00000140525.17	0.6
UHRF1	ENSG00000276043.4	0.6
FBXO5	ENSG00000112029.9	0.6
H2AFZ	ENSG00000164032.11	0.59
CENPU	ENSG00000151725.11	0.59
RAD54L	ENSG00000085999.11	0.59
NCAPG2	ENSG00000146918.19	0.59
DNMT1	ENSG00000130816.14	0.59
STMN1	ENSG00000117632.20	0.59
TMPO	ENSG00000120802.13	0.58
KIF4A	ENSG00000090889.11	0.58
PRC1	ENSG00000198901.13	0.58
NCAPH	ENSG00000121152.9	0.58
CENPK	ENSG00000123219.12	0.58
HMGN2	ENSG00000198830.10	0.58
ASPM	ENSG00000066279.16	0.58
KIF18B	ENSG00000186185.13	0.58
KIF11	ENSG00000138160.5	0.57
CHAF1B	ENSG00000159259.7	0.57
SKA1	ENSG00000154839.9	0.57
TCF19	ENSG00000137310.11	0.57
DONSON	ENSG00000159147.17	0.57
BUB1	ENSG00000169679.14	0.57
CCNB2	ENSG00000157456.7	0.57
CHEK1	ENSG00000149554.12	0.57
MCM2	ENSG00000073111.13	0.57
PSMC3IP	ENSG00000131470.14	0.57
SGOL2	ENSG00000163535.17	0.57

KIF23	ENSG00000137807.13	0.57
MCM5	ENSG00000100297.15	0.56
E2F1	ENSG00000101412.12	0.56
CDC45	ENSG00000093009.9	0.56
ASF1B	ENSG00000105011.8	0.56
CENPF	ENSG00000117724.12	0.56
CDCA5	ENSG00000146670.9	0.56
TUBA1B	ENSG00000123416.15	0.56
NUF2	ENSG00000143228.12	0.56
CDC25C	ENSG00000158402.18	0.56
CCNA2	ENSG00000145386.9	0.56
BRIP1	ENSG00000136492.8	0.56
MND1	ENSG00000121211.7	0.56
LRR1	ENSG00000165501.16	0.56
ZWINT	ENSG00000122952.16	0.56
TUBB	ENSG00000196230.12	0.55
CENPO	ENSG00000138092.10	0.55
SPC25	ENSG00000152253.8	0.55
POLA2	ENSG00000014138.8	0.55
H2AFV	ENSG00000105968.18	0.55
TPX2	ENSG00000088325.15	0.55
E2F2	ENSG00000007968.6	0.55
BIRC5	ENSG00000089685.14	0.55
SGOL1	ENSG00000129810.14	0.55
RFC2	ENSG00000049541.10	0.55
EXO1	ENSG00000174371.16	0.55
NEIL3	ENSG00000109674.3	0.55
EXOSC9	ENSG00000123737.12	0.55
PHF19	ENSG00000119403.13	0.55
FBXO43	ENSG00000156509.13	0.55
DLGAP5	ENSG00000126787.12	0.55
ZNF367	ENSG00000165244.6	0.55
KIF20A	ENSG00000112984.11	0.54
MXD3	ENSG00000213347.10	0.54
TIMELESS	ENSG00000111602.11	0.54
MAD2L1	ENSG00000164109.13	0.54
PRIM1	ENSG00000198056.13	0.54
CDT1	ENSG00000167513.8	0.54
UBE2T	ENSG00000077152.9	0.54
HJURP	ENSG00000123485.11	0.54
CKAP2L	ENSG00000169607.12	0.54
FAM64A	ENSG00000129195.15	0.54
FAM72B	ENSG00000188610.12	0.54
RNASEH2A	ENSG00000104889.4	0.54
GINS1	ENSG00000101003.9	0.54
METTL4	ENSG00000101574.14	0.53
NASP	ENSG00000132780.16	0.53
DTL	ENSG00000143476.17	0.53
RFC5	ENSG00000111445.13	0.53
TMPO-AS1	ENSG00000257167.2	0.53
DSN1	ENSG00000149636.15	0.53